Adaptive Divergence in Experimental Populations of *Pseudomonas fluorescens*. V. Insight into the Niche Specialist Fuzzy Spreader Compels Revision of the Model *Pseudomonas* Radiation

Gayle C. Ferguson,*,[1] Frederic Bertels,[†,2] and Paul B. Rainey[†,‡]

*Institute of Natural and Mathematical Sciences, [†]New Zealand Institute for Advanced Study and Allan Wilson Centre for Molecular Ecology and Evolution, Massey University Albany, Auckland 0745, New Zealand, and [‡]Max Planck Institute for Evolutionary Biology, Plön 24306, Germany

ABSTRACT *Pseudomonas fluorescens* is a model for the study of adaptive radiation. When propagated in a spatially structured environment, the bacterium rapidly diversifies into a range of niche specialist genotypes. Here we present a genetic dissection and phenotypic characterization of the fuzzy spreader (FS) morphotype—a type that arises repeatedly during the course of the *P. fluorescens* radiation and appears to colonize the bottom of static broth microcosms. The causal mutation is located within gene *fuzY* (*pflu0478*)—the fourth gene of the five-gene *fuzVWXYZ* operon. *fuzY* encodes a β-glycosyltransferase that is predicted to modify lipopolysaccharide (LPS) O antigens. The effect of the mutation is to cause cell flocculation. Analysis of 92 independent FS genotypes showed each to have arisen as the result of a loss-of-function mutation in *fuzY*, although different mutations have subtly different phenotypic and fitness effects. Mutations within *fuzY* were previously shown to suppress the phenotype of mat-forming wrinkly spreader (WS) types. This prompted a reinvestigation of FS niche preference. Time-lapse photography showed that FS colonizes the meniscus of broth microcosms, forming cellular rafts that, being too flimsy to form a mat, collapse to the vial bottom and then repeatably reform only to collapse. This led to a reassessment of the ecology of the *P. fluorescens* radiation. Finally, we show that ecological interactions between the three dominant emergent types (smooth, WS, and FS), combined with the interdependence of FS and WS on *fuzY*, can, at least in part, underpin an evolutionary arms race with bacteriophage SBW25Φ2, to which mutation in *fuzY* confers resistance.

ADAPTIVE radiation—the rapid emergence of phenotypic and ecological diversity within an expanding lineage—is among the most striking of evolutionary phenomena (Darwin 1859; Lack 1947; Dobzhansky 1951; Simpson 1953; Schluter 2000; Kassen 2009; Losos 2010). Fueled by competition and facilitated by ecological opportunity, successive radiations have shaped much of life's diversity. Of central importance are the phenotypic innovations that fashion the fit between organism and environment (Schluter 2000).

doi: 10.1534/genetics.113.154948
Manuscript received June 30, 2013; accepted for publication September 16, 2013; published Early Online September 27, 2013.
Supporting Information is available online at http://www.genetics.org/lookup/suppl/doi:10.1534/genetics.113.154948/-/DC1.
[1]Corresponding author: INMS, Massey University Albany, Private Bag 102904, North Shore Mail Centre, Auckland 0745, New Zealand. E-mail: g.c.ferguson@massey.ac.nz
[2]Present address: Biozentrum, University of Basel, CH-4056 Basel, Switzerland.

Understanding the nature of these innovations and the pathways by which they emerge and rise to prominence—often in parallel across estranged populations experiencing similar environments—is a central issue (Colosimo *et al.* 2005; Bantinaki *et al.* 2007; Conte *et al.* 2012). How mutational processes generate the variation presented to selection (McDonald *et al.* 2009; Braendle *et al.* 2010), how genetic architecture underpinning extant phenotypes determines the capacity of lineages to generate new and adaptive phenotypes (Poole *et al.* 2003; Wagner and Zhang 2011), and how ecological factors drive phenotypic divergence (Schluter 2009) are questions of seminal interest.

The relative simplicity of microbial systems, their capacity for rapid evolutionary change, and advances in technology that enable detailed genotypic traceability offer a unique opportunity to log moment-by-moment change in experimental populations, with the potential to contribute to

understanding of how genotype shapes phenotype, how phenotype interplays with the environment, and how environment may shape genotype (Mortlock 1982; Lenski *et al.* 1998; Rainey *et al.* 2000; Beaumont *et al.* 2009; Buckling *et al.* 2009; Blount *et al.* 2012; Hindré *et al.* 2012). In the context of adaptive radiation, the bacterium *Pseudomonas fluorescens* SBW25 has served as a useful model (reviewed within MacLean 2005 and Kassen 2009). When propagated in a spatially structured environment, SBW25 rapidly diversifies into a range of niche specialist genotypes. Smooth (SM) genotypes colonize the broth of static broth microcosms; wrinkly spreader (WS) genotypes colonize the air–liquid (AL) interface in the form of a self-supporting biofilm (or "mat"), via the overexpression of an acetylated cellulose-like polymer (ACP); and fuzzy spreaders (FS) form large, spreading colonies and appear to occupy the microcosm floor (Rainey and Travisano 1998). These three dominant types and their variants are maintained over time in serially propagated microcosms by the virtue of negative frequency-dependent interactions: each genotype is fittest when rare and fallible when common.

Previous work has defined the underlying mutational bases of WS genotypes (Spiers *et al.* 2002; Goymer *et al.* 2006; Bantinaki *et al.* 2007; McDonald *et al.* 2009), identified a set of mutational pathways that evolution repeatedly follows to generate this adaptive type (Rainey and Rainey 2003), and explained why evolution follows a subset of all possible pathways (McDonald *et al.* 2009). But what of fuzzy spreader? These morphotypes take longer to appear, but like WS, they arise repeatedly (Rainey and Travisano 1998). While WS is well understood, little is known about the ecology and genetics of FS. Here we describe the mutational causes of the FS phenotype, delineate the genetic route from genotype to phenotype to fitness, and unravel the links between FS physiology and the causes of its ecological specialization.

Materials and Methods

Bacterial strains, growth conditions, and manipulation

The ancestral (wild-type) SM strain is *P. fluorescens* SBW25 (PBR368) that was isolated from the leaf of a sugar beet plant grown at the University Farm, Wytham, Oxford, in 1989 (Rainey and Bailey 1996). The niche-specialist archetypal FS genotype (PBR367) was derived from the ancestral genotype after 7 days of selection in a spatially structured microcosm (Rainey and Travisano 1998). The niche-specialist WS genotype (PBR366; $wspF_{236\text{insGACCGTC}}$) was derived from the ancestral genotype after 3 days of selection in a spatially structured microcosm (Rainey and Travisano 1998). The *awsX* mutant WS_T (PBR656; $awsX_{\Delta 229\text{-}261}$) and the *mwsR* mutant WS_Z (PBR662; $mwsR_{G3055A}$) were similarly derived (McDonald *et al.* 2009). SBW25-Tn*7*-*lacZ* (PBR760), FS-Tn*7*-*lacZ* (PBR761), SBW25-$fuzY_{T443G}$::Tn*7*-*lacZ* (PBR762), SBW25Δ*fuzY*::Tn*7*-*lacZ* (PBR763), and FS-$fuzY_{wt}$::Tn*7*-*lacZ* (PBR764) derivatives used in Figure 2 competition assays carry a chromosomal insertion of mini-Tn*7*-*lacZ* (Choi *et al.* 2005). The strain FS-*lacZ* (PBR742) used in competition assays has a promoterless *'lacZ* inserted within the defective prophage locus of the chromosome (Zhang and Rainey 2007). Both the *'lacZ* and Tn*7*-*lacZ* markers are neutral with respect to fitness. A full list of strains and plasmids used in this study is given in Supporting Information, Table S1. The 112 independent FS genotypes FS3–FS214b were obtained by propagating the ancestral SM genotype (PBR368) in 214 independent spatially structured microcosms (Table S2). Microcosms were diluted and plated onto King's medium B (KB) agar after 5 days incubation and (except where otherwise indicated) a single FS genotype was selected at random from each microcosm. These genotypes were streaked for single colonies to check purity and then stored at −80°. In cases where two or more distinct fuzzy-like morphotypes were apparent, representatives of each genotype were selected and stored; these are indicated by "a", "b", etc. (Table S2).

P. fluorescens strains were cultured at 28° in KB (King *et al.* 1954). *Escherichia coli* strains were grown in LB at 37°. Antibiotics and supplements were used at the following concentrations: ampicillin, 100 $\mu g \cdot ml^{-1}$; cycloserine, 800 $\mu g \cdot ml^{-1}$; gentamicin, 10 $\mu g \cdot ml^{-1}$; kanamycin, 100 $\mu g \cdot ml^{-1}$; spectinomycin, 100 $\mu g \cdot ml^{-1}$; and tetracycline, 20 $\mu g \cdot ml^{-1}$. 5-Bromo-4-chloro-3-indolyl-β-D-galactopyranoside (X-gal) was added at a concentration of 60 $\mu g \cdot ml^{-1}$. *N*-[5-nitro-2-furfurylidene]-1-arminutesohy-dantoin was used to counterselect *E. coli* (100 $\mu g \cdot ml^{-1}$ in agar plates). Plasmid DNA was introduced to *E. coli* by transformation and *P. fluorescens* by transformation or conjugation, following standard procedures. The helper plasmid pRK2013 was used to facilitate conjugative transfer between *E. coli* and *P. fluorescens* (Figurski and Helinski 1979).

Molecular biology techniques

Standard molecular biology techniques were used throughout (Sambrook *et al.* 1989). Gateway technology (vector pCR8; Invitrogen, Carlsbad, CA) was used to clone PCR fragments. The fidelity of all cloned fragments was checked by DNA sequencing (Macrogen, Seoul, South Korea). Oligonucleotide primers for allelic replacements and reconstructions were designed on the basis of the SBW25 genome sequence (Silby *et al.* 2009).

Construction of deletion mutants and allelic replacements

A two-step allelic exchange strategy was used as described previously (Rainey 1999; Bantinaki *et al.* 2007). For the generation of deletion mutants, oligonucleotide primers were used to amplify ~1000-nucleotide regions flanking the gene(s) of interest. A third PCR reaction was used to join flanking sequences by splicing overlap extension (Horton *et al.* 1989). The product was cloned into pCR8 (and sequenced to check for errors); the resulting fragment was

excised using *Bgl*II or *Spe*I and introduced into the suicide vector pUIC3 (Rainey 1999). Deletion constructs were mobilized into *P. fluorescens* by conjugation and allowed to recombine with the chromosome by homologous recombination. Recombinants from which pUIC3 had been lost were identified from LB agar plates after a brief period of nonselective growth in KB broth (Kitten *et al.* 1998). To generate allelic replacements, PCR fragments (~3 kb) centered upon the allele of interest were cloned as above and introduced into pUIC3, and the replacement was made by recombination. Deletion and allelic exchange mutants were confirmed by PCR; allelic exchange mutants were further checked by DNA sequencing.

Gene complementation

A DNA fragment encoding *fuzY* (*pflu0478*) flanked by *Nde*I and *Bam*HI restriction sites was amplified by PCR and ligated with pCR8. The resultant plasmid was purified from *E. coli* transformants and the integrity of the insert confirmed by Sanger sequencing (Macrogen). For expression in *P. fluorescens*, *fuzY* was excised from pCR8 and ligated between the *Nde*I and *Bam*HI sites of expression vector pSX encoding *lacIq* and an IPTG-inducible *tac* promoter (Owen and Ackerley 2011). *P. fluorescens* transformants were purified by streaking to single colonies and the presence of the desired construct was confirmed by PCR.

Fitness of genotypes

Competitive fitness of FS genotypes was determined by direct competition between each FS genotype and FS (PBR367), FS-*lacZ* (PBR742), or FS-Tn*7*-*lacZ* (PBR761). Competitive fitness of SM genotypes was determined by direct competition between each SM genotype and SM (PBR368), SBW25-*lacZ* (PBR743), or SBW25-Tn*7*-*lacZ* (PBR760). Figure 2 fitness assays composed of six independent replicate contrasts used reciprocal strain marking as follows: in three replicate assays the reference strain (SBW25 or FS) was marked with mini-Tn*7*-*lacZ*, and in three replicate assays the reconstructed mutant strain was marked with mini-Tn*7*-*lacZ*, thus nullifying any effect of the marker on competition. Competitive fitness of WS genotypes was determined by direct competition between each WS genotype and WS mutant LSWS-Tn*7*-*lacZ* ($wspF_{A901C}$; PBR741). All strains were grown overnight in shaken KB broth before introduction into spatially structured or unstructured microcosms (~10^5 cells of each competitor) at a ratio of 1:1. Relative fitness was calculated as the ratio of Malthusian parameters of the genotypes being compared (Lenski *et al.* 1991).

Experimental evolution

Cells from −80° glycerol stocks were streaked onto KB agar plates to produce isolated single colonies. Populations were founded by inoculation of 6 ml KB broth in glass microcosms with a single representative colony from these KB plates; replicate populations were derived from independent single colonies. Populations were incubated at 28° in structured (static) microcosms. Propagation of populations occurred at regular intervals (of duration stated in *Results*) by transfer of a mixed sample (6 μl) to a fresh microcosm. At the time of each transfer, samples were spread onto KB plates to screen for colonies (~500–1500) with a different morphology (for example, WS or FS or SM, as stated in *Results*). Representative colonies of new emergent types were streaked to single colonies on KB plates to confirm heritability and purity prior to propagation in liquid culture and storage at −80°.

Sequencing and sequence analysis

Whole-genome resequencing of the entire 6.7-Mbp genome of the archetypal FS isolate (PBR367) was achieved using Illumina Solexa technology. Paired-end sequencing was performed in two channels for 76 cycles on an Illumina GAIIx with a paired-end module. The data were analyzed using the Illumina OLB pipeline v1.8: the total cluster number was 58,919,811 with 38,328,187 clusters passing filter (65%). Reads were aligned to the *P. fluorescens* SBW25 genome sequence (Silby *et al.* 2009), using SOAP2; a single SNP (T443G) was identified after extracting all SNPs from regions covered by >10 sequence reads with a PHRED quality >20 and where 95% of the aligned nucleotides agreed. The presence of the T443G SNP in FS and its absence in SBW25 was confirmed by Sanger sequencing (Macrogen). Analyses of regions upstream and downstream of *fuzY*, including the identification of orthologous genes in *Pseudomonas* species, were performed using Artemis 14.0.0 (Rutherford *et al.* 2000) and the Generic Genome Browser (GBrowse) version 2.37 (Stein *et al.* 2002) within the *Pseudomonas* Genome Database (Winsor *et al.* 2009).

fuzY from 112 independently isolated FS isolates was amplified by PCR and sequenced by the Sanger method (Macrogen). DNA sequences were analyzed using Sequencher 4.10.1 (Gene Codes) or Geneious 5.5.6 (Biomatters) software.

Phage resistance assays

Sensitivity of SBW25 mutants to bacteriophage SBW25Φ2 was determined by pipetting 5-μl droplets of diluted phage lysate onto lawns of bacterial cells overlaid onto KB plates. Bacterial overlays were prepared by mixing 200 μl of bacterial cells from an overnight culture with 3 ml of molten top agar (KB with 0.8% agar). Phage sensitivity was scored as the presence of clear zones or individual plaques on bacterial lawns after 24-hr incubation at 28°.

Imaging

Niche preference in structured microcosms: Six ml of KB broth in glass microcosms was inoculated with ~5×10^5 bacteria and incubated at 28° without shaking for 48 hr (unless otherwise indicated). Structured microcosms were photographed with a Canon PowerShot G7 camera.

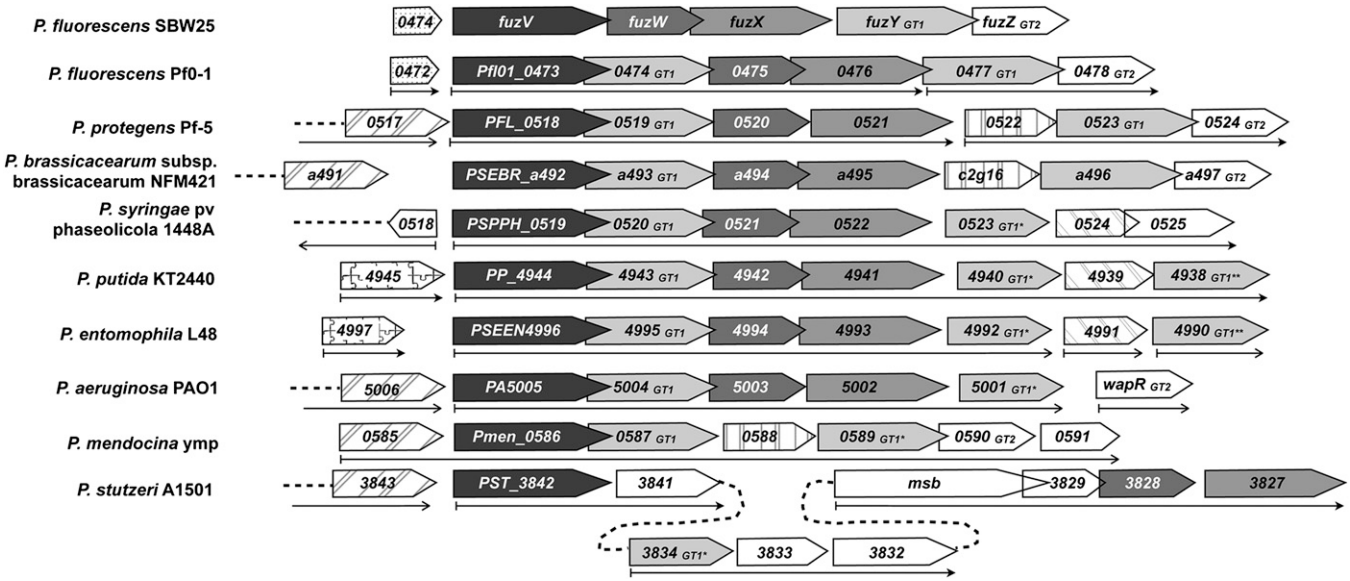

Figure 1 Comparison of the arrangement of genes at the fuzzy spreader locus in *Pseudomonas* species. The predicted fuzzy spreader operon in *P. fluorescens* SBW25 comprises five genes with predicted functions relating to LPS modification: *fuzV* (537,073–538,830) encodes a predicted carbamoyl transferase (NodU family), *fuzW* (538,831–539,727) encodes a putative transcriptional regulator (Mig-14 family), *fuzX* (539,697–541,124) encodes a predicted deacetylase, *fuzY* (541,184–542,332) encodes a predicted β-glycosyltransferase (GT1 family), and *fuzZ* (542,329–543,210) encodes a predicted α-glycosyltransferase (GT2 family). Many of the genes within this hypothetical operon have highly conserved orthologs within a range of *Pseudomonas* species. Orthologous genes were identified by Reciprocal Best Blast Analysis/Ortholuge performed upon data collated in the *Pseudomonas* Genome Database and are grouped by shade (or pattern). * and ** indicate glycosyltransferases of different GT1 ortholog groups. Open boxes indicate genes with no orthologs within the regions depicted. Overlapping boxes indicate ORFs that initiate within the coding sequence of the upstream ORF. Thin arrows indicate computationally predicted operons from the Database of prOkaryotic OpeRons (DOOR), where available.

Movies of bacterial growth in structured microcosms over time were produced: Six ml of KB broth in glass microcosms was inoculated with $\sim 5 \times 10^5$ bacteria and incubated at 28° without shaking. Bacterial growth was recorded by time-lapse photography, using a Canon PowerShot G7 camera and PSRemote (Version 1.9.1) Camera Control software (Breeze Systems, Camberley, Surrey, UK): photographs were taken at 5- or 10-min intervals over 24- to 72-hr periods and compiled into movies, using Microsoft Movie Maker (Version 5.1).

Colony morphology: Bacteria from a 10^6-fold dilution of an overnight KB culture were spread onto KB plates and incubated at 28° for 48 hr. Colony morphology was examined and photographed using a Zeiss Stemi 2000-C dissection microscope fitted with a Canon PowerShot A640 digital camera.

Results

The fuzzy spreader phenotype is caused by a single nonsynonymous mutation in a putative lipopolysaccharide modification gene

The FS morphotype has proved intractable to standard genetic analysis. Repeated attempts to locate the causal loci by suppressor analysis have failed. We therefore sequenced the genome of an archetypal FS mutant (PBR367). Comparison of the FS genome with the SBW25 reference genome identified a single-nucleotide polymorphism within *pflu0478* (a T to G transversion at position 443), a gene predicted to encode a putative glycosyltransferase involved in modification of surface lipopolysaccharides (LPS). The SNP caused the substitution of valine for glycine at position 148 ($\text{Pflu0478}_{\text{V148G}}$). *pflu0478* is located in a predicted operon of five genes (*pflu0475–pflu0479*) that are likely transcribed as a single unit (Figure 1). These genes are hereafter designated as *fuzVWXYZ* for "***fuz***zy spreader locus". The predicted functions of these gene products relate to LPS modification: *fuzV* (537,073–538,830) encodes a predicted carbamoyl transferase (NodU family), *fuzW* (538,831–539,727) encodes a hypothetical protein with a predicted acetyltransferase domain (NAT_SF superfamily, *E*-value: 2.31*e*-10) with significant similarity to the Mig-14 family of antimicrobial resistance proteins (*E*-value: 2.03*e*-150), *fuzX* (539,697–541,124) encodes a predicted deacetylase, *fuzY* (541,184–542,332) encodes a predicted β-glycosyltransferase (GT1 group), and *fuzZ* (542,329–543,210) encodes a predicted α-glycosyltransferase (GT2 group). The *fuz* locus was previously identified in a suppressor analysis of WS types and shown to be required for expression of the WS phenotype (McDonald *et al.* 2009), indicating a genetic link between WS and FS phenotypes. A summary of the diguanylate cyclase (DGC)-encoding pathways underpinning the evolution of the WS phenotype is given in Figure S1.

Orthologs of *fuzVWXYZ* were identified across a range of *Pseudomonas* species (Figure 1). The structure of the 5′ end

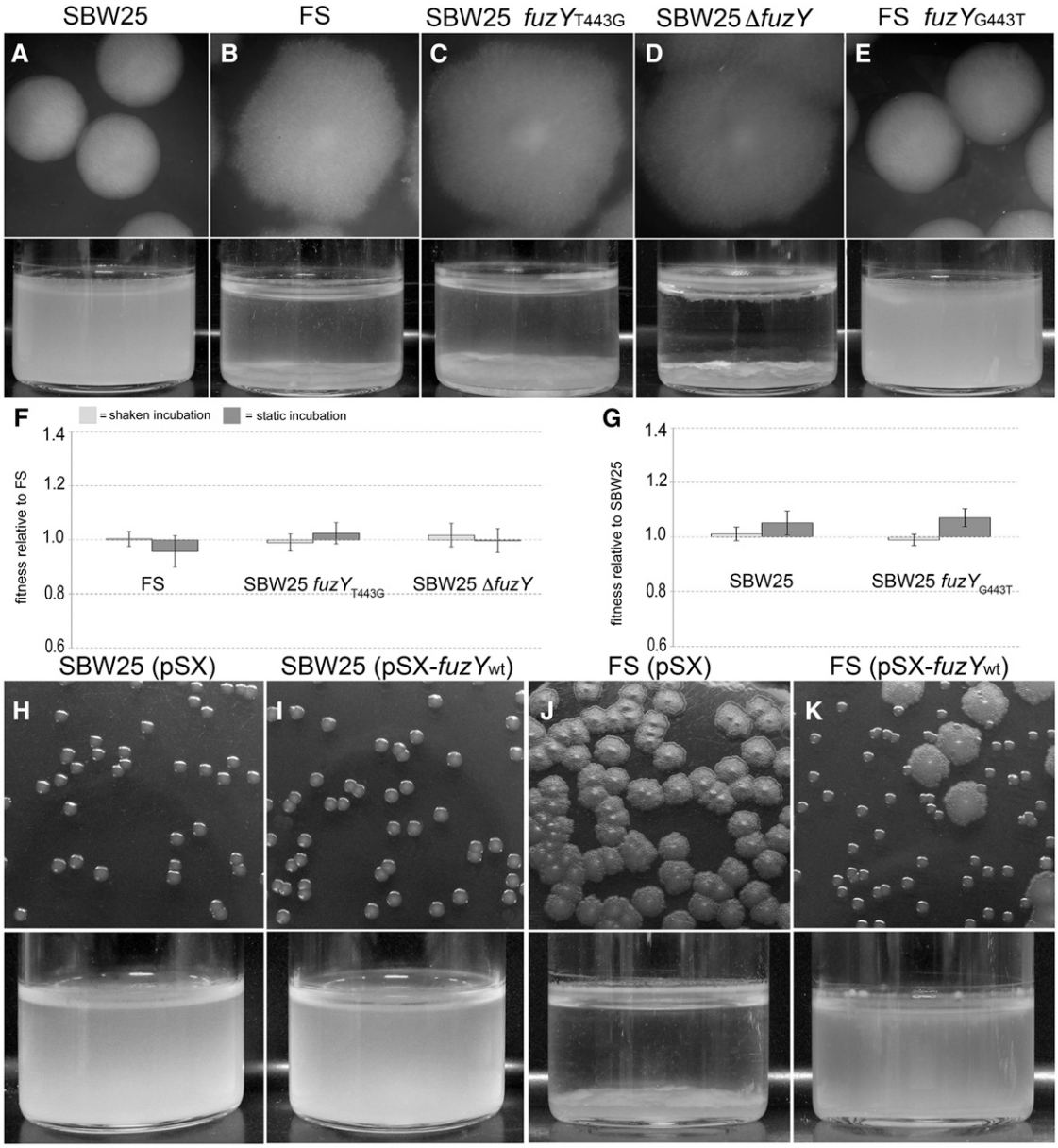

Figure 2 Mutation of *fuzY* causes the fuzzy spreader (FS) phenotype. (B–D) $fuzY_{T443G}$ and Δ*fuzY* mutations reconstructed in SBW25 gave a phenotype indistinguishable from FS. (A and E) Reconstruction of the wild-type *fuzY* sequence in FS gave a phenotype indistinguishable from SBW25. Top panels show 48-hr colonies on KB plates. Bottom panels show growth after 48 hr of incubation in structured KB microcosms. (F and G) Fitness of the reconstructed mutants was measured relative to *lacZ*-marked derivatives of FS (F) or SBW25 (G) (see *Materials and Methods*) with either shaken (bars with light shading) or static incubation (bars with dark shading). No statistically significant fitness differences were measured between native and reconstructed FS mutants under any conditions [one-way ANOVA: $P = 0.5048$ (shaken), $P = 0.4406$ (static)]. Similarly, fitness differences between native and reconstructed SBW25 were not statistically significant [Dunnett's test: $P = 0.0745$ (shaken), $P = 0.5727$ (static)]. Fitness measures are a ratio of Malthusian parameters and are the mean of six independent replicates; error bars show standard error of the mean. (H–K) $fuzY_{T443G}$ (carried by FS) was complemented by overexpression of the wild-type *fuzY* gene in *trans* from the vector pSX.

of the operon (*fuzVWX*) is highly conserved across all species, except for the more distantly related *P. stutzeri*. It is likely that the ancestral operon included an additional GT1-group glycosyltransferase between *fuzV* and *fuzW*. In contrast, the 3′ end of the operon is more fluid: for most species, orthologs of *fuzVWX* are coupled with an assortment of glycosyltransferases.

The region upstream of *fuzV* is poorly conserved. Orthologs of the upstream genes are present in many pseudomonads but only in *P. fluorescens* SBW25 and Pf0-1 is there juxtaposition of *pflu0474*—encoding a short hypothetical protein of unknown function—and *fuzV* (Figure 1); in most other species *pflu0474* is linked to the permease component of a putative ABC-type multidrug transport system. This

indicates that *pflu0474* is not a component of the fuzzy spreader operon.

Loss-of-function mutations in fuzY generate fuzzy spreaders

To test whether the T443G substitution is alone sufficient to cause the FS phenotype, the mutation was reconstructed in a naive SBW25 background. The resultant mutant—SBW25-*fuzY*$_{T443G}$ (PBR744)—expressed a fuzzy colony morphology on KB plates and exhibited the archetypal fuzzy spreader growth pattern within structured microcosms (Figure 2, A–C). Similarly, reconstruction of the wild-type sequence in FS (FS-*fuzY*$_{wt}$, PBR752) generated a mutant with a smooth colony morphology that grew within the broth phase (Figure 2E). To determine whether the FS phenotype is a consequence of loss of function, *fuzY* was cleanly deleted, taking care to retain the first codon of *fuzZ*: SBW25Δ*fuzY* (PBR745) also displayed the typical FS colony morphology and pattern of growth in structured microcosms (Figure 2D). Both SBW25-*fuzY*$_{T443G}$ and SBW25Δ*fuzY* were comparable to FS in fitness when competed against a marked FS derivative in both shaken (unstructured) and static (spatially structured) microcosms (Figure 2, F and G).

If the FS phenotype is the simple consequence of a loss-of-function mutation in *fuzY*, restoration of the ancestral phenotype should be achieved by expression of *fuzY* in *trans*. Indeed, complementation of *fuzY*$_{T443G}$ by overexpression of *fuzY*$_{wt}$ from vector pSX (PBR753) resulted in restoration of the ancestral phenotype (Figure 2, J and K). Overexpression of *fuzY*$_{wt}$ in ancestral SBW25 (PBR751) produced no discernible effect on either phenotype or growth (Figure 2, H and I).

A single genetic route confers the fuzzy spreader phenotype through a diverse range of fuzY mutations

To determine whether mutation of *fuzY* is the sole cause of all fuzzy morphotypes we isolated 112 FS and FS-like morphotypes from independent spatially structured microcosms and classified them on the basis of colony morphology. By visual inspection, two distinct classes of spreading colonies, fuzzy in appearance, were discernible. "Typical" fuzzy spreaders (88 isolates) were rough textured and opaque in appearance, with irregular colony margins. "Atypical" fuzzy spreaders (aFS) (24 isolates) were of a similar form, but differed from the typical class in colony opacity and/or texture. Similarly, an inspection of niche occupancy revealed differences between the classes: FS types failed to grow within the broth phase, appearing as a "volcano-like" biomass on the microcosm floor (as in Figure 2, B and C). In contrast, aFS types grew within the broth phase, with many producing weak mats.

For each of the 112 isolates, we sequenced *fuzY*: 92 isolates harbored mutations; of these, 88 were of the typical class, and 4 were of the aFS class. The remaining 20 genetically uncharacterized isolates were of the aFS class and phenotypically distinct from FS. These could be further partitioned into two groups on the basis of their susceptibility to bacteriophage SBW25Φ2 (Table S2). Thus, aFS aside, the mutational basis of the FS phenotype appears to be simple, with a diverse range of mutations from SNPs causing nonsynonymous substitutions or nonsense mutations to insertions and deletions (indels) of various lengths causing frameshifts throughout the length of the gene (Table 1, Table S2).

Table 1 Spectrum of *fuzY* mutations isolated

Mutational class (bp)	Unique mutations (no. mutants)
SNPs	
Transitions	10 (14)
AT > GC	2 (2)
GC > AT	8 (12)
Transversions	13 (40)
AT > CG	1 (28)
GC > TA	6 (6)
AT > TA	2 (2)
GC > CG	4 (4)
Indels	
+1 insertions	5 (6)
+2 insertions	2 (2)
−1 deletions	10 (10)
−2 deletions	4 (4)
Small insertions (5–8)	2 (2)
Large insertions (951)	2 (2)
Small deletions (3–6)	4 (4)
Large deletions (24–3373)	7 (8)
Total	59 (92)

Of the 112 independent FS and FS-like mutants isolated, 92 harbored mutations within *fuzY*. The mutations ranged from SNPs causing missense or nonsense mutations to small and large deletions and insertions (indels) causing frameshifts throughout the length of the gene. Numbers not in parentheses indicate the number of unique mutations isolated, while numbers in parentheses indicate the total number of mutants isolated for each class. T443G occurred 28 times (31% of all mutants), C565T occurred twice, C622T occurred three times, G857A occurred twice, and Δ882–947 occurred twice. Of the seven large deletions, two extended into *fuzZ* and one deleted all of *fuzX* and *fuzY* and some of each of *fuzW* and *fuzZ*. Of the large insertions, one resulted from the duplication of adjacent sequence and the other from the insertion of a putative transposon encoded elsewhere in the genome. Mutant genotypes are listed in full in Table S2.

Of 92 independent *fuzY* causal mutations, 54 were SNPs at 23 unique positions (Table 1). Of the 23 unique SNPs, 10 were transitions (predominantly GC > AT) and 13 were transversions (predominantly GC > TA and GC > CG); 16 were missense mutations and 7 were nonsense. Interestingly, more than one-quarter of all the independently isolated fuzzy spreaders were caused by an identical SNP—the same T443G transversion carried by the resequenced "archetypal" isolate—causing valine to be substituted for glycine at position 148 in the protein (V148G). Similar single-site mutation biases have been reported elsewhere and explained by replication template switching within imperfect repeat (quasi-palindromic) sequences during DNA replication (De Boer and Ripley 1984; Mo *et al.* 1991; Demarini *et al.* 1998; Viswanathan *et al.* 2000; Lovett 2004). A comparison of the DNA sequence surrounding the T443G "hotspot" with nearby sequences failed to identify any imperfect palindromic matches likely to template a T > G substitution at position 443.

Table 2 Description of *fuzY* mutations within independent FS isolates included in Figure 3

Isolate[a]	Class	Nucleotide change	Amino acid change
8	FS	Δ4 (−1 Fs[b])	M1Δ (37)[c]
73	FS	Δ28–33	ΔLQ
104	sFS	268insT (+1 Fs)	F90Δ (4)
133	sFS	C288G (Tv[b])	N96K
156b	sFS	G352T (Tv)	G118W
145b	sFS	T376A (Tv)	Y126N
108	sFS	432insCCTGGCGG	R144Δ (14)
FS	FS	T443G (Tv)	V148G
152	FS	Δ568–569 (−2 Fs)	A190Δ (93)
143	FS	G620T (Tv)	G207V
56	aFS	A638G (Ts[b])	K213R
163	FS	Δ638–639 (−2 Fs)	I212Δ (71)
12	sFS	C662A (Tv)	A221E
117a	FS	*fuzY*Δ770–1149, *fuzZ*Δ1–220	T256Δ (220), ΔFuzZ
145a	sFS	809ins126nt (duplication of 126 nt immediately upstream of insertion point)	Y271Δ (153)
44	FS	G857A (Ts)	G286D
191	FS	951ins Tn *pflu2158*, *pflu4347*, *pflu5832*, or *pflu4873*	G318Δ (10)
192b	aFS	C947A (Tv)	A316E
111b	aFS	G953A (Ts)	G318D
142	FS	1059insT (+1 Fs)	R353Δ (19)

[a] Isolates are ordered by position of mutation (5′–3′ direction); mutant genotypes are listed in full in Table S2.
[b] Fs, frameshift; Tv, transversion; Ts, transition.
[c] Numbers in parentheses indicate the number of amino acid residues from the mutation site until the predicted STOP codon.

Of the 92 mutations, 28 were small indels at 27 unique positions. The majority of these can be explained by nascent strand misalignment [slipped-strand mispairing (Levinson and Gutman 1987)] within monotonic nucleotide "runs" (14 of 28), by duplication of adjacent sequence (2 of 28), or by deletion of a directly repeated sequence (2 of 28). How the remaining 12 small indels were created is not clear but, notably, one mutant (FS126a; Table S2) had acquired a single-base-pair insertion producing a perfect 5-bp inverted repeat of the adjacent sequence, potentially a consequence of intramolecular template switching (Lovett 2004). Five of 92 mutants were caused by large deletions within *fuzY* [Δ629–760, Δ775–896, Δ862–885, and Δ882–947 (which occurred twice)]; two of 92 mutants had deletions extending from the 3′ end of *fuzY* into *fuzZ*; and one mutant had a deletion extending from the 3′ end of *fuzW* to the 5′ half of *fuzZ*. The remaining mutant was caused by the insertion of a transposon encoded elsewhere in the genome.

Typical FS isolates are indistinguishable from each other in terms of colony morphology; however, subtle differences in phenotype are conferred by different mutations within *fuzY*. When the independent FS isolates were screened for niche preference in spatially structured microcosms, most isolates were indistinguishable from the archetypal FS ($fuzY_{T443G}$; PBR367). However, a subset of seven FS isolates exhibited a small amount of growth within the broth phase in addition to producing biomass on the microcosm floor. The mutations responsible for these "subtle" isolates (sFS) were located in two or three distinct regions of the gene: codons 90–144, codon 221, and codon 271—four were missense substitutions and three were insertions of 1, 8, and 126 nucleotides, respectively. Three of the four aFS isolates with mutations within *fuzY* carried missense substitutions—two located close together (A316E and G318D) and a third (K213R) located nearby sFS mutant A221E (Table S2). The fourth aFS mutant had a large deletion extending from *fuzW* into *fuzZ*.

To further explore the possible phenotypic differences among *fuzY* mutants, we carried out fitness assays on a selection of independent FS mutations (Table 2), including the seven sFS genotypes and three of the aFS genotypes. Small fitness differences were detected between some pairs of *fuzY* mutants when competed in spatially structured microcosms; however, the variance between replicates—attributable to the tendency of the competitors to diversify into a range of niche specialists over the 3-day period of the assay—was large (Figure 3A). Competition assays performed in unstructured microcosms, by way of a comparison, revealed a greater number of statistically significant fitness differences (Figure 3B). In general, mutants differing in fitness to archetypal FS generally corresponded to those with sFS or aFS phenotypes. However, fitness measured in unstructured microcosms mapped poorly to that measured in structured microcosms. Surprisingly, we observed significant differences in the ability of some fuzzy isolates to diversify (predominantly into a range of WS types) during static incubation (Figure 3C); this subset of rapidly diversifying types belongs exclusively to the aFS and sFS classes and in some instances these correspond to those with significantly different fitness as measured under shaken incubation (Figure 3B). When fitness and diversity measures were pooled by mutant class

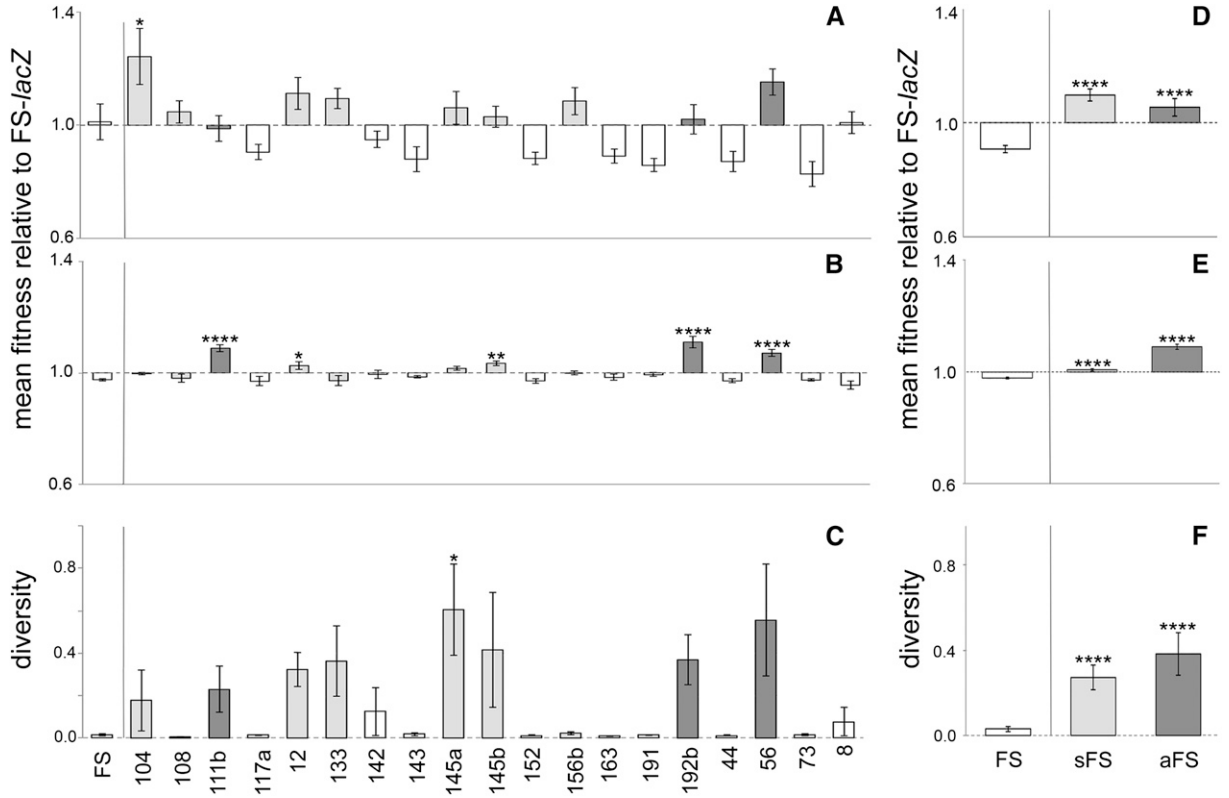

Figure 3 Relative fitness and diversification of independent FS isolates after 3 days incubation in spatially structured or unstructured environments. Fitness was measured relative to a *lacZ*-marked derivative of FS (PBR742). Typical FS mutants (open bars) display the archetypal fuzzy colony morphology and accumulate at the bottom of structured microcosms. Subtle FS mutants (bars with light shading) display the archetypal fuzzy colony morphology and accumulate at the bottom of microcosms but also grow to a degree within the broth phase. Atypical FS mutants (bars with dark shading) display colony morphology intermediate between FS and SM and grow within the broth phase of structured microcosms. (A–E) Fitness measures are a ratio of Malthusian parameters and are the mean of six independent replicates; error bars show standard error. Asterisks indicate statistically significant contrasts in comparison to the archetypal FS isolate PBR367 (multiple-comparisons tests as shown: $*P \leq 0.05$, $**P \leq 0.01$, $***P \leq 0.001$, $****P \leq 0.0001$). For competitions within spatially structured environments (A), differences in mean fitness for some pairs of mutants were statistically significant (Welch's ANOVA, $P = 0.0001$), although only mutant 104 was significantly fitter than the archetypal FS ($P = 0.0109$, Dunnett's multiple-comparisons test). For competitions within unstructured environments (B), differences in mean fitness for some pairs of mutants were statistically significant (Welch's ANOVA, $P = 0.0001$); mutants 111b, 12, 145b, 192b, and 56 were significantly fitter than the FS archetype ($P < 0.0001$, $= 0.034$, $= 0.0075$, < 0.0001, < 0.0001, respectively, Dunnett's multiple-comparisons test). (C) Population diversification was measured as the proportion of colonies whose morphology deviated from the ancestral type after 72 hr static incubation; values represent a mean of six independent replicates and error bars show standard error. Differences in diversification for some pairs of mutants were statistically significant (Welch's ANOVA, $P \leq 0.0281$), although only mutant 145a diversified to a significantly greater extent than the archetypal FS ($P = 0.0025$, Dunn's multiple-comparisons test). When the data for individual mutants were pooled by FS classification, the contrasts were strongly significant [(D–F) Welch's ANOVA: $P < 0.0001$]. For competitions in spatially structured environments (D), the sFS and aFS groups were of equal fitness but each was significantly more fit than the FS group ($P < 0.0001$, Dunnett's multiple-comparisons test). For competitions in unstructured environments (E), each group mean was significantly different to every other group mean, with aFS being the fittest group and FS the least fit ($P < 0.0001$, Tukey's multiple-comparisons test). Similarly, the sFS and aFS groups both diversified to a significantly greater extent than the FS group [(F) $P < 0.0001$, Dunn's multiple comparisons test].

(FS *vs.* sFS *vs.* aFS), the trends were marked: for competitions in structured microcosms, aFS and sFS were equally fit and significantly fitter than FS (Figure 3D). For competitions in unstructured microcosms, aFS were significantly fitter than sFS, which were significantly fitter than FS (Figure 3E). Similarly, when the propensity of isolates to diversify was compared by mutant class, the sFS and aFS groups diversified to a significantly greater extent than the FS group (Figure 3F).

Taken together, the data suggest that although the majority of mutations within *fuzY* confer phenotypically indistinguishable fuzzy morphologies—most likely the consequence of loss of function of the enzyme—some *fuzY* mutations confer a more subtle phenotype. It is likely that the aFS and sFS groups express partially functional FuzY enzymes and consequently display cell surface properties intermediate to those of FS and SM. The greater propensity of aFS and sFS types to diversify in structured microcosms is likely attributable to the fact that the gene retains some functionality and that this functionality is required for expression of other niche specialist types, in particular WS.

Table 3 Phenotypes of *fuzVWXYZ* single-gene knockout mutants

Mutant	Colony morphology[a]	Niche occupancy[b] (static microcosm)	SBW25Φ2 sensitivity[c]
Δ *fuzV*	Small, smooth	Broth phase (slow growth)	Resistant
Δ *fuzW*	Smooth (like SM)	Broth phase	Resistant (rough)
	Rough	Microcosm floor	Sensitive (smooth)
Δ *fuzX*	Smooth (like SM)	Broth phase	Sensitive
Δ *fuzY*	Fuzzy spreader	Microcosm floor	Resistant
Δ *fuzZ*	Large, smooth[d]	Broth phase	Resistant
Δ *fuzVWXYZ*	Small, smooth	Microcosm floor (slow growth)	Resistant

[a] Colony morphologies were scored after 48 hr growth on KB plates.
[b] Niche occupancy was scored after 72 hr growth in 6 ml KB microcosms at 28°.
[c] All mutants were tested for sensitivity to SBW25Φ2.
[d] The *fuzZ* mutant appears as a fuzzy spreader when cultured on LBA plates.

Genes fuzVWXYZ encode phenotypically related functions, contributing to the modification of cell surface structures

Having mapped the full spectrum of FS mutations exclusively to *fuzY*, we sought to determine the contribution of flanking genes. Deletion of the entire operon (*fuzVWXYZ*) generated a small-colony variant (Table 3, Figure 4). With the exception of *fuzX*, all single-gene deletion mutants gave rise to colonies with distinct phenotypes (Table 3, Figure 4); however, only deletion of *fuzY* generated the FS phenotype. Notable was the *fuzW* mutant, which reproducibly generated colonies of both "rough" (PBR746-R) and "smooth" morphotypes (PBR746-S) (Figure 4).

Revision of the FS niche preference

The explanatory model for the maintenance of niche specialist types arising during the course of the *Pseudomonas* radiation involves negative frequency-dependent interactions between SM, WS, and FS arising from the emergence of trade-offs due to diversifying selection. This model is based on data from reciprocal "invasion from rare" experiments combined with observation of the niche preference of the three dominant types: SM colonizes the broth phase, WS the AL interface, and FS the microcosm floor (Rainey and Travisano 1998). While the existence of frequency-dependent interactions among the primary types is firmly established, there is reason to reexamine the niche preference of FS. This stems from the fact that oxygen is removed from the broth phase by the founding genotype within the first 12 hr of growth (B. Ibelings and P. B. Rainey, unpublished data; Koza *et al.* 2010), leading to the seemingly contradictory observation that FS, evolved from the obligate aerobe SBW25, apparently grows in an environment with no oxygen. It is difficult to imagine how LPS modification might confer the property of anaerobic growth upon FS. To further investigate the connection between genotype and phenotype we revisited the question of FS niche occupancy. Structured microcosms were inoculated with FS cells and their growth was recorded by time-lapse photography (File S1). As expected, no substantial growth of FS took place in the broth phase, unlike that observed in microcosms seeded with ancestral SBW25 (File S2). Instead, the first visually discernible growth took place at the meniscus, with small rafts of cells observed to propagate both inward toward the center of the AL interface and downward in a stalactite-like fashion (File S1). As these rafts increase in size, they fall from the interface to the floor of the microcosm as snowflakes, but repeatedly reform. No substantial biofilm ever forms at the surface, but growth clearly occurs. Thus FS, like WS, specializes in colonizing the AL interface, albeit by a distinctively different strategy. Rather than forming a mat via the production of adhesive polymers (Spiers *et al.* 2002, 2003), FS

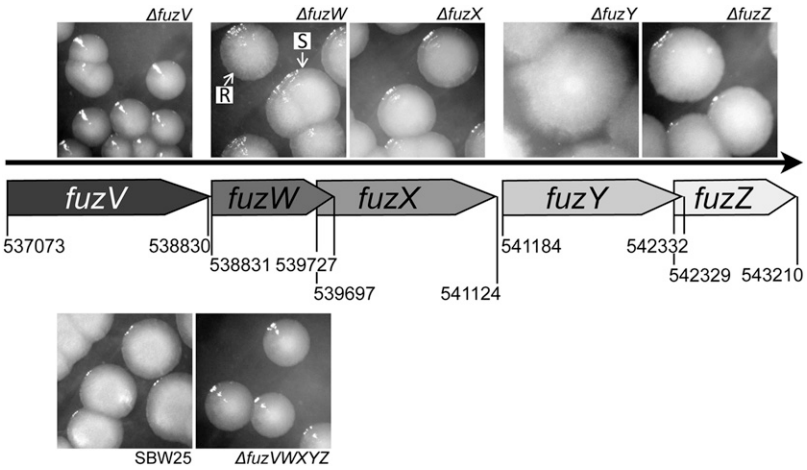

Figure 4 Colony morphologies of single *fuz* gene deletion mutants and a *fuzVWXYZ* deletion mutant. Deletion of the *fuzVWXYZ* operon produced a small-colony variant, distinct in phenotype from both FS and SM, indicating that one or more of the genes surrounding *fuzY* also contribute to cell surface characteristics. Each single-gene deletion (except for *fuzX*) produced a mutant with distinctly altered colony morphology, unlike either FS or SM (Table 3). Deletions were constructed in a SBW25 background via a two-step allelic exchange strategy as described previously (Rainey 1999; Bantinaki *et al.* 2007). Base numbers refer to the SBW25 genome sequence [NC_012660.1 (Silby *et al.* 2009)]. Images show 48-hr colonies on KB plates.

Table 4 The effect of pH on the growth of *P. fluorescens*

A.	pH	FS: mean CFU·ml^{-1} ± SEM (*P*-value)	SBW25 Δ*fuzY*: mean CFU·ml^{-1} ± SEM (*P*-value)
	6.5	$8.7 \times 10^8 \pm 1.3 \times 10^8$ (0.0733)	$1.2 \times 10^9 \pm 5.3 \times 10^8$ (0.3213)
	7.0	$5.5 \times 10^8 \pm 4.9 \times 10^7$	$5.7 \times 10^8 \pm 1.3 \times 10^8$
	7.5	$4.9 \times 10^8 \pm 1.4 \times 10^8$ (0.7372)	$3.8 \times 10^8 \pm 1.3 \times 10^8$ (0.3578)
	8.0	$6.5 \times 10^8 \pm 1.3 \times 10^7$ (0.1084)	$6.7 \times 10^8 \pm 7.9 \times 10^7$ (0.5265)
	8.5	$5.9 \times 10^8 \pm 1.3 \times 10^8$ (0.7403)	$8.6 \times 10^8 \pm 2.9 \times 10^8$ (0.4047)
B.	pH	FS: pH prior to growth	SBW25 Δ*fuzY*: pH after growth
	6.5	6.55 ± 0.01	8.21 ± 0.09
	7.5	7.60 ± 0.03	8.61 ± 0.10
	8.5	8.27 ± 0.03	8.86 ± 0.07

(A) Rows give the viable titer (as CFU·ml^{-1}) of FS and SBW25 Δ*fuzY* in 6-ml KB microcosms of differing pH following 72 hr static incubation at 28°. (B) The pH of KB was measured postautoclaving but prior to inoculation with FS. Inoculated microcosms were incubated statically at 28° for 72 hr. Spent media were sterilized by filtration through 0.22-μm filters and the pH was again measured. Titers and pH measurements are a mean of three independent replicates and variance is given as the standard error of the mean. *P*-values are derived from unpaired *t*-tests comparing the titer at each pH with that at pH 7. No statistically significant differences were found for any of the contrasts.

forms transient rafts due to changes in a cell surface component.

To explore the basis of the *fuzY*-dependent raft-forming behavior the flocculating ability of FS cells was examined by growing cells for 3 days in structured microcosms (SM and WS were included as controls). Cells were then dispersed into suspension by vortex mixing and incubated statically for a further 24 hr, with the addition of tetracycline to prevent further growth. Time-lapse photography revealed rapid flocculation of FS cells with an almost complete clearing of the broth phase within 12 hr (File S3). In contrast, SBW25 and WS cells remained largely in suspension. From this we conclude that clumping is mediated by cell–cell attraction and is not a consequence of failure of mother and daughter cells to disperse following cell division. That flocculation requires specific interactions between FS cells is supported by the observation that the ancestral (SM) genotype does not flocculate and remains in suspension when mixed 1:1 with FS in statically incubated microcosms (data not shown).

Although FS grows poorly in the broth phase of structured microcosms, growth sometimes occurs after several days of incubation. As SBW25 is known to modify its growth environment with a resultant increase in pH over time (Table 4B), we speculated that the tendency for FS to form flocs might be pH dependent. To test the effect of pH on growth and flocculation, we recorded (again by time-lapse photography) the growth of FS across a range of pHs from 6.5 to 8.5 (File S4). At pH 8 and above, growth occurred predominantly in the broth phase. At pH 7.5, growth occurred initially at the AL interface, with rafts of cells falling to the microcosm floor, but after 24 hr the broth phase began to cloud with growth. Broth phase growth was less marked at pH 7 and did not occur at pH 6.5. The pH-dependent differences in FS growth were not due to an effect of pH on growth rate: populations were titered at 72 hr and cell density (as CFU·ml^{-1}) did not differ between treatments (Table 4A). Similarly, postgrowth flocculation of dispersed cells occurred only at low pH (File S5). From this we conclude that the failure of FS to grow freely in the broth phase of structured microcosms is a consequence of flocculation following cell separation and that the particular cell surface characteristics that promote flocculation are charge mediated.

fuzY mutation in WS results in a compromised ability to form mats

The *fuzVWXYZ* locus was previously identified as a suppressor of the WS phenotype in the **l**arge **s**preading **w**rinkly **s**preader (LSWS; $wspF_{A901C}$) and **a**lternate **w**rinkly **s**preader (AWS; *awsX* Δ100–138) mutants (McDonald *et al.* 2009; Figure S1), suggesting a genetic link between the WS and FS phenotypes. To explore this further, $fuzY_{T443G}$ and Δ*fuzY* mutations were reconstructed in a $wspF_{236insGACCGTC}$ background (WS; PBR366). The resulting mutants were compromised in their ability to form substantive mats at the AL interface: WS-$fuzY_{T443G}$ (PBR754) and WSΔ*fuzY* (PBR755) mutant colonies show a decreased wrinkled appearance on KB plates and produce feeble mats (fWS) that readily collapse to the microcosm floor (Figure 5B). Comparison of mat growth over time revealed striking differences between WS and WS-$fuzY_{T443G}$: WS mat formation initiates with the appearance of cell aggregates at the AL interface, which in time grow together to form a thin but robust film, interspersed with denser aggregates of rope-like growth (File S6). In contrast, WS-$fuzY_{T443G}$, while also initiating growth at the AL interface, forms "rafts", many of which fall to the microcosm floor. Over time these rafts expand to form a dense mat of surface growth, this, however, being unstable with the periodic appearance of "holes" as biomass drops to the microcosm floor. No networks of rope-like structures were observed. Mat strength was measured by the glass bead assay (Rainey and Rainey 2003). Whereas 3-day-old WS mats were able to support an average of 0.24 ± 0.07 g of 2-mm glass beads (0.01 g) before collapsing, WS-Δ*fuzY* mats were unable to support even a single bead. Wild-type mat formation and

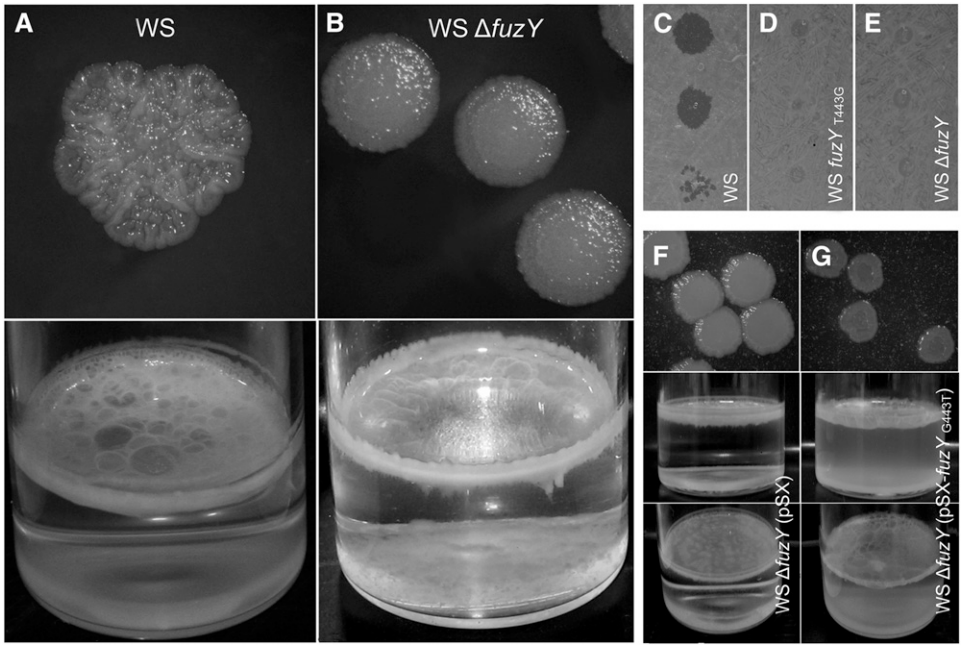

Figure 5 *fuzY* mutation in LSWS compromises mat integrity. (A and B) $fuzY_{T443G}$ (not shown) and Δ*fuzY* mutations reconstructed in WS (PBR366) produced colonies with a decidedly less wrinkled appearance and, although to the eye capable of forming a thick mat at the AL interface, produced weak mats incapable of supporting 2-mm glass beads (top panels show 48-hr colonies on KB plates; bottom panels show growth after 48-hr static incubation in KB microcosms). (C–E) Phage SBW25Φ2 can plaque on WS (C) but not on either WS-$fuzY_{T443G}$ (PBR754) (D) or WS Δ*fuzY* (PBR755) (E). (F and G) $fuzY_{T443G}$ was complemented by overexpression of the wild-type *fuzY* gene in *trans* from the vector pSX (top panels show 48-hr colonies on KB plates; middle and bottom panels show growth after 48-hr static incubation in KB microcosms).

wrinkled colony morphology were restored to WS-Δ*fuzY* by overexpression of $fuzY_{wt}$ from pSX (PBR756; Figure 5, F and G). As with SBW25, overexpression of $fuzY_{wt}$ in WS (PBR757) produced no discernible effect on either phenotype or growth or the ability to support beads (data not shown).

In contrast to FS, the genetic routes to WS are many and varied, with mutation within three distinct diguanylate cyclase-containing pathways (*Wsp*, *Aws*, and *Mws*) conferring cellulose overproduction and a mat-forming phenotype (McDonald *et al.* 2009; Figure S1). However, deletion of *fuzY* had the same phenotypic effect on each of three distinct WS genotypes (PBR755, PBR758, and PBR759; data not shown). Thus, the putative LPS defect caused by loss of FuzY function has consequences for the downstream effect of the WS mutations, most likely the secretion and arrangement of acetylated cellulose polymers, rather than a specific interaction with the particular genes or protein components encoded by the *wsp* operon (Spiers and Rainey 2005).

$fuzY_{T443G}$ confers resistance to SBW25Φ2

A previously noted feature of fuzzy spreader genotypes is their resistance to the lytic bacteriophage SBW25Φ2. Droplets of phage suspension produce clear zones on lawns of SBW25 but no clearing is observed on lawns of FS (Figure 6). All typical FS isolates, including the sFS subclass and SBW25Δ*fuzY*, are phage resistant (Table S2). Interestingly, the three broth-dwelling aFS isolates with mutations within *fuzY* are also phage resistant. We conclude that all (known) mutations in *fuzY* confer resistance to phage, regardless of any other effects of the mutations on niche preference. Single deletions of genes *fuzVWX* and *fuzZ* (but not *fuzX*) also conferred resistance to SBW25Φ2 (Table 3). Rough *fuzW* mutants (PBR746-R) are phage resistant whereas smooth *fuzW* mutants (PBR746-S) are phage sensitive.

Location of the FS causal mutation to a gene product predicted to modify LPS allows us to speculate upon the Φ2 receptor: LPS serves as a receptor for a broad range of bacteriophage in many bacterial species (for examples see Michel *et al.* 2010; Filippov *et al.* 2011; Garbe *et al.* 2011; Shin *et al.* 2012). It appears likely that phage resistance in FS is conferred by alterations in LPS structure. SBW25Φ2 proteins involved in phage attachment and entry are most closely related to *P. aeruginosa*-specific ΦKMV-like phages of the T7 supergroup, including ΦLKA1 (BLASTp, data not shown). Notably, ΦLKA1 infection requires expression of *algC* (Ceyssens *et al.* 2011)—a gene encoding phosphoglucomutase, required for the synthesis of a complete lipopolysaccharide core (Coyne *et al.* 1994).

An evolutionary arms race at the FS locus

The fact that *fuzY* mutations confer resistance to bacteriophage SBW25Φ2 but have deleterious pleiotropic consequences for subsequent evolution of WS—the superior competitor at the AL interface (Rainey and Travisano 1998)—raises the possibility that a trade-off between phage resistance and FS *vs.* WS strategies to colonize the AL interface might underlie—at least in part—the previously reported arms race between *P. fluorescens* SBW25 populations and SBW25Φ2 (Buckling and Rainey 2002a). Such a possibility can be envisaged as follows: in the absence of phage the ancestral SM genotype rapidly diversifies into numerous niche specialist types, including WS and FS. Presence of phage selects for phage-resistant genotypes, in particular, FS morphotypes, while at the same time selecting against phage-sensitive genotypes such as WS. As FS types increase in frequency, the phage titer—under a serial transfer regime—declines. Once at low density, opportunity exists for the competitively superior WS types to reemerge—either

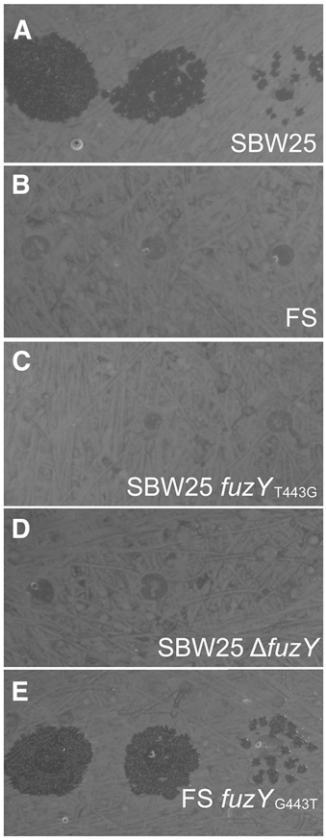

Figure 6 $fuzY_{T443G}$ confers resistance to SBW25Φ2. (A–E) Phage SBW25Φ2 forms plaques on *P. fluorescens* SBW25 (A) and the reconstructed wild-type FS-$fuzY_{G443T}$ (E) but is unable to form plaques on *fuzY* mutants (B–D).

from preexisting sensitive types or, *de novo*, by mutation, from the dominant FS population. However, for WS to evolve from FS, a mutation that reverts (or compensates for) the *fuzY* mutation is required. Given that FS and WS share dependence on a functional *fuz* operon, it is possible that the bacterial response to the presence of phage may involve continual cycling between phage-sensitive WS and phage-resistant FS, effected by mutational changes at the *fuzY* locus.

We explored this possibility by asking whether WS genotypes can evolve from FS and, if they do, whether the FS-derived WS are phage sensitive. Fifty-six independent FS mutants representative of the range of *fuzY* mutational types were propagated for 3-day periods by serial dilution in structured microcosms until the emergence of colony morphologies resembling WS types (Table S3). All (except for 3) FS genotypes gave rise to WS types within four serial transfers (with WS emergence most commonly requiring just one or two successive transfers to detect). However, the majority of the derived types produced feeble mats (fWS), indicative of the fact that the *fuzY* mutation had neither been reversed nor compensated for by a change restoring functionality to the *fuz* locus. Consistent with this thesis, most weak fWS types remained phage resistant (Table S3). However, strong mat-forming WS derivatives (typical of regular WS mats) did arise from a number of FS isolates and repeatedly arose from 2 FS isolates in particular: FS108 ($fuzY_{432insCCTGGCGG}$) and FS156a ($fuzY_{C1096T}$) (Table S2). These derived WS types were phage sensitive. A more extensive collection of FS-derived WS genotypes was selected from 12 replicate populations of each of FS108 and FS156a after 5 days growth in structured microcosms (data not shown). Sequencing of *fuzY* from 22 phage-sensitive FS108-derived WS isolates revealed a reversion to the wild-type sequence (by retraction of an 8-bp duplication of adjacent sequence at base pair 432) in every case. Sequencing of *fuzY* from 17 phage-sensitive FS156a-derived WS isolates revealed a reversion of C1096T to the wild-type T1096C in 7 cases (restoring a Gln codon from an amber stop) and an additional SNP (A1097G) in 10 cases (creating a Trp codon from an amber stop). Taken together, these data demonstrate that while fWS are more likely to evolve from FS (probably by a single mutation), true WS do emerge and are most likely the consequence of two mutations: the first one reverting the *fuzY* gene to wild type (and thus generating the SM morph), followed by a second mutation—in the *wsp*-, *aws*-, or *mws*-determined pathways (McDonald *et al.* 2009)—to give WS. The extent to which this is possible is likely to depend on the nature of the FS-causing *fuzY* mutation. Certain *fuzY* mutations, by virtue of their genetic context (for example, those involving expansion or contraction of repeated sequence) are more likely to revert than others. When reversion of *fuzY* occurs, phage-sensitive WS are inevitable and are likely competitively superior to phage-resistant fWS: the relative fitness of fWS (WS-$fuzY_{T443G}$) in 3-day structured microcosms was just 0.80 ± 0.06 whereas the relative fitness of WS was 0.97 ± 0.05 (*t*-test: $P < 0.0001$, $n = 8$). The strong mat-forming WS is substantially fitter than weak mat-forming WS-$fuzY_{T443G}$ and the major component of the differential fitness is the ability to exploit the AL interface when competed in a structured environment. Thus, given sufficient generational time, it is predicted that phage-sensitive WS types will derive from FS progenitors in spatially structured environments once the dominance of FS genotypes has driven SBW25Φ2 to near extinction.

An on-going arms race requires that phage-sensitive WS can generate phage-resistant FS by mutation. From knowledge of the underlying genetics this is highly probable, but is likely to require two mutations: one to revert the WS to SM and a second to generate FS. From 12 replicate populations of each of three distinct FS-derived WS genotypes propagated for two successive 3-day periods and three successive 7-day periods by serial dilution in structured microcosms, 23 produced FS at detectable frequencies, with earlier emergence of "step one" SM and/or fWS types as predicted (Table S4). All of the derived FS types were phage resistant. Thus, the plausibility of a continuing arms race with changes wrought at the *fuzY* locus is demonstrated.

Discussion

How mutational processes create the molecular variation upon which natural selection acts is a question readily addressed by experimental evolution (Beaumont *et al.* 2009; Blount *et al.* 2012). Ultimately, we seek to complete a comprehensive account of the common evolutionary trajectories during *P. fluorescens* SBW25 adaptive radiation and understand the underlying genetic architecture, mutational processes and targets, and the emergent ecological interactions that drive adaptive evolution. Here, we have described the genetic and ecological bases of FS fitness. Moreover, our genetic analyses have led to a reassessment of the niche preference of FS and the ecological processes underpinning the *Pseudomonas* radiation.

The FS mutational spectrum

Previous work has cataloged the underlying mutational bases of WS genotypes and identified the number of mutational routes to the WS phenotype (Spiers *et al.* 2002; Goymer *et al.* 2006; Bantinaki *et al.* 2007; McDonald *et al.* 2009). While a multitude of pathways lead to WS, the genetic underpinnings of FS are much simpler. Nevertheless, our catalog of FS mutants provides useful information about the mutational processes that generate the diversity upon which natural selection acts. The spectrum of FS causal mutations is highly diverse—encompassing SNPs causing both missense and nonsense mutations, small indels causing frameshifts, and both small and large deletions—with mutations spaced throughout the length of the gene. A number of studies, both experimental and comparative, have reported mutational spectra across genes and genomes in bacterial lineages experiencing hard or soft selection (Miller 1985; Leong *et al.* 1986; Mo *et al.* 1991; Garibyan *et al.* 2003; and reviewed in Ochman 2003; Wolff *et al.* 2004). More recently, experimental evolution studies, long-term experiments in particular, have provided the material for cataloging mutational spectra—both neutral and those subject to positive selection—across whole genomes (Wielgoss *et al.* 2011; Lee *et al.* 2012). These studies reveal commonalities (such as a general twofold bias for transitions over transversions, in particular the G:C > A:T substitution) but also idiosyncrasies. Indeed it can be difficult to compare mutational spectra between species, and even between genes within the same species, since mutation rates and classes are affected by gene-specific parameters such as distance of the gene from the replication origin, the direction of transcription relative to the passage of a replication fork, and the level of transcription (reviewed by Ochman 2003; Juurik *et al.* 2012).

Various studies have reported mutational spectra for single genes encoding proteins constrained by functions essential for viability (Garibyan *et al.* 2003; Wolff *et al.* 2004), making it difficult to draw conclusions about the relative occurrence of SNPs and indels and the six classes of substitution. Although it may be difficult, perhaps impossible, to infer how the mutations sampled in this study might compare with the full spectrum of *fuzY* mutations occurring through time in each evolving population, the mutations we sampled (at least those of the typical FS class) did not differ markedly in their relative fitness, indicating a phenotypic equivalence. Knowing that all confer a similar phenotype, it is possible to argue that the spectrum of sampled mutations is likely to be largely representative of the broader pool of those occurring in *fuzY* sequence space. Considering unique SNPs only, the transition:transversion (Ts:Tv) ratio in our study was 1:1.3. Considering the transitions, the distribution of AT > GC and GC > AT substitutions (after correcting for GC content) did not differ from that expected by chance ($\chi^2 = 1.517$, $P = 0.2180$, d.f. = 1, chi-square test). Similarly, the relative frequencies of the four possible transversions did not differ from that expected ($\chi^2 = 2.000$, $P = 0.5724$, d.f. = 3, chi-square test).

Curious is the finding that one-quarter of all the independently isolated fuzzy spreaders were caused by an identical SNP—the same T443G transversion carried by the resequenced archetypal isolate—causing valine to be substituted for glycine at position 148 (V148G). Fitness assays performed under conditions similar to those in which our independent FS isolates evolved show that this mutation does not confer a fitness benefit substantially greater than that of any other FS mutation; indeed, mathematical models conclude that the differential fitness necessary to account for the preferential selection of T443 is beyond biological reality (E. Libby, unpublished results). The more frequent occurrence of this mutation suggests that it has an increased probability of being generated, likely as a consequence of the local DNA sequence or secondary structure. A comparison of the DNA sequence surrounding the T443G hotspot with nearby sequences failed to identify any imperfect palindromic matches likely to template a T > G substitution at position 443; thus replication template switching within imperfect repeat (quasi-palindromic) sequences during passage of a replication fork is not obviously behind the generation of T443G (De Boer and Ripley 1984; Mo *et al.* 1991; Demarini *et al.* 1998; Viswanathan *et al.* 2000; Lovett 2004).

Ecological interactions underpinning the Pseudomonas radiation

How genetic diversity translates into phenotypic diversity and how phenotypic diversity in turn drives the interactions between species and their environment is of considerable interest. The interplay of predominant emergent types during *P. fluorescens* SBW25 radiations has been extensively described (Rainey and Travisano 1998; Rainey and Rainey 2003; Rainey 2005). However, closer inspection of FS growth within spatially structured microcosms—motivated initially by the overlap of the genetic architecture underpinning both FS and WS—has led to a significant revision of our understanding of the ecology of this particular morphotype: previously designated a bottom dweller, FS innocula observed over time initially begin growth at the AL interface, with flocs

of cells attempting to spread as a biofilm but ultimately falling to the microcosm floor. This pattern of growth indicates that FS competes with WS for occupancy of the AL interface, which fits with the fact that oxygen is the primary limiting resource driving the *Pseudomonas* radiation. FS performs poorly in competition with WS (Rainey and Travisano 1998; Rainey 2005); however, it repeatedly arises and increases in frequency whenever spatially structured microcosms are seeded with the ancestral type. Moreover, that aFS and sFS types repeatedly arise in parallel adaptive radiations implies an ecological complexity within the simple structured broth microcosm that remains to be fully described. Our working model is as follows: growth of the ancestral SM genotype rapidly depletes the environment of oxygen, which establishes conditions that favor evolution of mat-forming WS types. WS mats dominate for several days before collapsing (Rainey and Rainey 2003). Mat collapse opens a niche for FS types, which exploit this opportunity via the formation of transient rafts that exist for sufficient time to enable FS cells to access oxygen that is otherwise absent from the microcosm. Interestingly, SM types, being unable to adhere to FS types, cannot hitchhike with FS and are thus unable to take advantage of FS rafts in the same way that they can take advantage of the WS mats. This accounts for the previously noted inhibitory effect of FS on SM (Rainey 2005): growth of FS takes oxygen from the uppermost layer of broth, thus depriving SM of this limiting resource. SM growth is subsequently compromised (Rainey 2005). Eventually WS types reinvade and perpetuate the cycle. Diversity is maintained by time-lagged frequency-dependent selection fueled by the fallibility of the surface-colonizing strategies of both WS and FS.

The effect of fuzY mutation on WS phenotype

The genetic link between FS and WS—the two key emergent types whose negative frequency-dependent interactions drive the dynamics within diversifying structured microcosms—is an unanticipated outcome of these studies. The *fuzVWXYZ* locus was previously identified as a suppressor of the LSWS ($wspF_{A901C}$) and AWS (*awsX* Δ100–138)-based WS morphotypes (McDonald *et al.* 2009), an association that was reconfirmed here. WS-$fuzY_{T443G}$ and WSΔ*fuzY* mutant colonies showed a decreased wrinkled appearance on KB and produced mats that collapsed easily to the microcosm floor.

The role of LPS as a major component of WS biofilm strength and integrity, as a consequence of interactions between LPS and the cellulose matrix of the biofilm, was revealed in an earlier study (Spiers and Rainey 2005) and is well supported (Lau *et al.* 2009; Nielsen *et al.* 2011; Nilsson *et al.* 2011). Alteration of the bacterial cell surface, with consequent changes to cell hydrophobicity, adhesive properties, and motility, likely perturbs the cell–cell interactions that maintain biofilm structure. The relationship between LPS defects and the adhesive, cohesive, and viscoelastic properties of biofilms and how these properties correlate with biofilm structure has been extensively characterized in *P. aeruginosa* PAO1 (Lau *et al.* 2009). Essentially, more dramatic LPS defects (such as full truncation of O antigen) result in stronger adhesion of cells to glass and other abiotic surfaces and stronger cell–cell interactions (evident by flocculation). Furthermore, mutants lacking O antigen produce biofilms with weaker viscoelastic properties. Recent studies with *P. putida* KT2440 EPS mutants support a model in which LPS mediates the necessary cell–cell interactions that maintain biofilm matrix stability following attachment (Nilsson *et al.* 2011), with EPS in a stabilizing role and cellulose polymers providing additional structural support (Nielsen *et al.* 2011; Nilsson *et al.* 2011).

An evolutionary arms race due to trade-offs in niche specialization

Phages are important determinants of microbial evolution and population structure (reviewed in Stern and Sorek 2010; Koonin and Wolf 2012). Their success in the face of asymmetry in the coevolutionary potential of phages, relative to that of their more complex bacterial hosts, raises questions as to their persistence (Lenski 1984). Various explanations have been put forward: one is that phages and their hosts participate in an on-going arms race mediated by endless cycles of bacterial mutations to phage resistance and phage counterdefenses (Rodin and Ratner 1983a,b). Evidence consistent with this comes from experiments with SBW25 and SBW25Φ2 (Buckling and Rainey 2002a,b; Brockhurst *et al.* 2004, 2006; Benmayor *et al.* 2008; Paterson *et al.* 2010; Gomez and Buckling 2011) and with other bacterial systems (for examples see Kashiwagi and Yomo 2011; Dennehy 2012; Levin *et al.* 2013; Seed *et al.* 2013). An alternative explanation posits that phages may persist if there exists a mixture of sensitive and resistant hosts where the resistant types are less fit in competition for resources than the sensitive types (Levin *et al.* 1977). Such a scenario stands to allow phage persistence if resistant bacteria revert to sensitivity and in so doing restore some capacity that is lost by the resistance-generating mutation (Lenski 1984). Such mutations would be likely once phages are rare, thus allowing phage reinvasion. This scenario appears to be relevant to our findings—at least in part—thus providing potential for persistent coevolution. Phage-sensitive WS are superior colonizers of the air–liquid interface; however, in the presence of phages their success is compromised: FS instead dominate. However, as phage titers decline (with declining availability of WS hosts), opportunity exists for mutants that revert to phage-sensitive, competitively superior, WS types. We show that this requires two mutations; nonetheless, such a possibility clearly exists.

The necessity of phage resistance in an environment where phages are abundant entails a trade-off against the optimal strategy for bacterial colonization: in the case of our simple experimental system, phage resistance is traded off against the ability to generate stable biofilms, enabling optimal access to O_2 for growth; in native environments, phage resistance is predicted to trade off against strategies

for the establishment of infection and colonization of host organisms—strategies typically mediated by bacterial surface structures. Indeed, O antigen is essential for the establishment of infection (or protection against host defenses) in a diverse array of plant and animal pathogens (Cava *et al.* 1989; Dekkers *et al.* 1998; Yang *et al.* 2000; Kannenberg and Carlson 2001; Poon *et al.* 2008; Kesawat *et al.* 2009); moreover, the O antigen serves as a receptor for phages (Michel *et al.* 2010; Filippov *et al.* 2011; Garbe *et al.* 2011; Shin *et al.* 2012). Thus it would appear that O antigens are subject to two conflicting selective pressures: pressure to change to avoid phage predation and pressure to be maintained to enable colonization of host species during infection. Such a trade-off may be widely relevant to persistence of phage and their bacterial hosts.

Acknowledgments

We thank members of the Rainey group for discussion and comments on the manuscript and Eric Libby for mathematical modeling. pSX was a gift from David Ackerley. Financial support was provided by the Foundation for Research, Science, and Technology; the Allan Wilson Centre; and Massey University. P.B.R. is a James Cook Research Fellow and gratefully acknowledges the Royal Society of New Zealand.

Literature Cited

Bantinaki, E., R. Kassen, C. G. Knight, Z. Robinson, A. J. Spiers *et al.*, 2007 Adaptive divergence in experimental populations of *Pseudomonas fluorescens*. III. Mutational origins of Wrinkly Spreader diversity. Genetics 176: 441–453.

Beaumont, H. J. E., J. Gallie, C. Kost, G. C. Ferguson, and P. B. Rainey, 2009 Experimental evolution of bet hedging. Nature 462: 90–93.

Benmayor, R., A. Buckling, M. B. Bonsall, M. A. Brockhurst, and D. J. Hodgson, 2008 The interactive effects of parasites, disturbance, and productivity on experimental adaptive radiations. Evolution 62: 467–477.

Blount, Z. D., J. E. Barrick, C. J. Davidson, and R. E. Lenski, 2012 Genomic analysis of a key innovation in an experimental *Escherichia coli* population. Nature 489: 513–518.

Braendle, C., C. F. Baer, and M.-A. Felix, 2010 Bias and evolution of the mutationally accessible phenotypic space in a developmental system. PLoS Genet. 6: e1000877.

Brockhurst, M. A., P. B. Rainey, and A. Buckling, 2004 The effect of spatial heterogeneity and parasites on the evolution of host diversity. Proc. Biol. Sci. 271: 107–111.

Brockhurst, M. A., A. Buckling, and P. B. Rainey, 2006 Spatial heterogeneity and the stability of host-parasite coexistence. J. Evol. Biol. 19: 374–379.

Buckling, A., and P. B. Rainey, 2002a Antagonistic coevolution between a bacterium and a bacteriophage. Proc. Biol. Sci. 269: 931–936.

Buckling, A., and P. B. Rainey, 2002b The role of parasites in sympatric and allopatric host diversification. Nature 420: 496–499.

Buckling, A., R. C. Maclean, M. A. Brockhurst, and N. Colegrave, 2009 The Beagle in a bottle. Nature 457: 824–829.

Cava, J. R., P. M. Elias, D. A. Turowski, and K. D. Noel, 1989 *Rhizobium leguminosarum* CFN42 genetic regions encoding lipopolysaccharide structures essential for complete nodule development on bean plants. J. Bacteriol. 171: 8–15.

Ceyssens, P.-J., T. Glonti, A. M. Kropinski, R. Lavigne, N. Chanishvili *et al.*, 2011 Phenotypic and genotypic variations within a single bacteriophage species. Virol. J. 8: 134–138.

Choi, K.-H., J. B. Gaynor, K. G. White, C. Lopez, C. M. Bosio *et al.*, 2005 A Tn*7*-based broad-range bacterial cloning and expression system. Nat. Methods 2: 443–448.

Colosimo, P. F., K. E. Hosemann, S. Balabhadra, G. J. Villarreal, M. Dickson *et al.*, 2005 Widespread parallel evolution in sticklebacks by repeated fixation of Ectodysplasin alleles. Science 307: 1928–1933.

Conte, G. L., M. E. Arnegard, C. L. Peichel, and D. Schluter, 2012 The probability of genetic parallelism and convergence in natural populations. Proc. Biol. Sci. 279: 5039–5047.

Coyne, M. J., Jr., K. S. Russell, C. L. Coyle, and J. B. Goldberg, 1994 The *Pseudomonas aeruginosa algC* gene encodes phosphoglucomutase, required for the synthesis of a complete lipopolysaccharide core. J. Bacteriol. 176: 3500–3507.

Darwin, C. R., 1859 *The Origin of Species*. John Murray, London.

de Boer, J. G., and L. S. Ripley, 1984 Demonstration of the production of frameshift and base-substitution mutations by quasi-palindromic DNA sequences. Proc. Natl. Acad. Sci. USA 81: 5528–5531.

Dekkers, L. C., A. J. van der Bij, I. H. Mulders, C. C. Phoelich, R. A. Wentwoord *et al.*, 1998 Role of the O-antigen of lipopolysaccharide, and possible roles of growth rate and of NADH:ubiquinone oxidoreductase (nuo) in competitive tomato root-tip colonization by *Pseudomonas fluorescens* WCS365. Mol. Plant Microbe Interact. 11: 763–771.

DeMarini, D. M., M. L. Shelton, A. Abu-Shakra, A. Szakmary, and J. G. Levine, 1998 Spectra of spontaneous frameshift mutations at the *hisD3052* allele of *Salmonella typhimurium* in four DNA repair backgrounds. Genetics 149: 17–36.

Dennehy, J. J., 2012 What can phages tell us about host-pathogen coevolution? Int. J. Evol. Biol. 2012: 396165.

Dobzhansky, T., 1951 *Genetics and the Origin of Species*. Columbia University Press, New York.

Figurski, D., and D. Helinski, 1979 Replication of an origin-containing derivative of plasmid RK2 dependent on a plasmid function provided *in trans*. Proc. Natl. Acad. Sci. USA 76: 1648–1652.

Filippov, A. A., K. V. Sergueev, Y. He, X. Z. Huang, B. T. Gnade *et al.*, 2011 Bacteriophage-resistant mutants in *Yersinia pestis*: identification of phage receptors and attenuation for mice. PLoS ONE 6: e25486.

Garbe, J., B. Bunk, M. Rohde, and M. Schobert, 2011 Sequencing and characterization of *Pseudomonas aeruginosa* phage JG004. BMC Microbiol. 11: 102.

Garibyan, L., T. Huang, M. Kim, E. Wolff, A. Nguyen *et al.*, 2003 Use of the *rpoB* gene to determine the specificity of base substitution mutations on the *Escherichia coli* chromosome. DNA Repair 2: 593–608.

Gomez, P., and A. Buckling, 2011 Bacteria-phage antagonistic coevolution in soil. Science 332: 106–109.

Goymer, P., S. G. Kahn, J. G. Malone, S. M. Gehrig, A. J. Spiers *et al.*, 2006 Adaptive divergence in experimental populations of *Pseudomonas fluorescens*. II. Role of the GGDEF regulator WspR in evolution and development of the Wrinkly Spreader phenotype. Genetics 173: 515–526.

Hindré, T., C. Knibbe, G. Beslon, and D. Schneider, 2012 New insights into bacterial adaptation through *in vivo* and *in silico* experimental evolution. Nat. Rev. Microbiol. 10: 352–365.

Horton, R., H. Hunt, S. Ho, J. Pullen, and L. Pease, 1989 Engineering hybrid genes without the use of restriction enzymes: gene splicing by overlap extension. Gene 77: 61–68.

Juurik, T., H. Ilves, R. Teras, T. Ilmjärv, K. Tavita *et al.*, 2012 Mutation frequency and spectrum of mutations vary at different chromosomal positions of *Pseudomonas putida*. PLoS ONE 7: e48511.

Kannenberg, E. L., and R. W. Carlson, 2001 Lipid A and O-chain modifications cause *Rhizobium* lipopolysaccharides to become hydrophobic during bacteroid development. Mol. Microbiol. 39: 379–391.

Kashiwagi, A., and T. Yomo, 2011 Ongoing phenotypic and genomic changes in experimental coevolution of RNA bacteriophage Qβ and *Escherichia coli*. PLoS Genet. 7: e1002188.

Kassen, R., 2009 Toward a general theory of adaptive radiation: insights from microbial experimental evolution. Ann. N. Y. Acad. Sci. 1168: 3–22.

Kesawat, M. S., B. K. Das, G. R. Bhaganagare, and V. Sharma, and Manorama, 2009 Isolation and characterization of lipopolysaccharides from different rhizobial isolates. J. Crop Sci. Biotechnol. 12: 109–113.

King, E. O., M. K. Ward, and D. E. Raney, 1954 Two simple media for the demonstration of pyocyanin and fluorescin. J. Lab. Clin. Med. 44: 301–307.

Kitten, T., T. G. Kinscherf, J. L. McEvoy, and D. K. Willis, 1998 A newly identified regulator is required for virulence and toxin production in *Pseudomonas syringae*. Mol. Microbiol. 28: 917–929.

Koonin, E. V., and Y. I. Wolf, 2012 Evolution of microbes and viruses: A paradigm shift in evolutionary biology? Front. Cell. Infect. Microbiol. 2: 119.

Koza, A., O. Moshynets, W. Otten, and A. J. Spiers, 2010 Environmental modification and niche construction: developing O_2 gradients drive the evolution of the Wrinkly Spreader. ISME J. 5: 665–673.

Lack, D., 1947 *Darwin's Finches*. Cambridge University Press, Cambridge, UK.

Lau, P. C. Y., T. Lindhout, T. J. Beveridge, J. R. Dutcher, and J. S. Lam, 2009 Differential lipopolysaccharide core capping leads to quantitative and correlated modifications of mechanical and structural properties in *Pseudomonas aeruginosa* biofilms. J. Bacteriol. 191: 6618–6631.

Lee, H., E. Popodi, H. Tang, and P. L. Foster, 2012 Rate and molecular spectrum of spontaneous mutations in the bacterium *Escherichia coli* as determined by whole-genome sequencing. Proc. Natl. Acad. Sci. USA 109: E2774–E2783.

Lenski, R. E., 1984 Coevolution of bacteria and phage: Are there endless cycles of bacterial defenses and phage counterdefenses? J. Theor. Biol. 108: 319–325.

Lenski, R., M. Rose, S. Simpson, and S. Tadler, 1991 Long-term experimental evolution in *Escherichia coli*. I. Adaptation and divergence during 2,000 generations. Am. Nat. 138: 1315–1341.

Lenski, R. E., J. A. Mongold, P. D. Sniegowski, M. Travisano, F. Vasi *et al.*, 1998 Evolution of competitive fitness in experimental populations of *E. coli*: What makes one genotype a better competitor than another? Anton. Leeuw. 73: 35–47.

Leong, P. M., H. C. Hsia, and J. H. Miller, 1986 Analysis of spontaneous base substitutions generated in mismatch-repair-deficient strains of *Escherichia coli*. J. Bacteriol. 168: 412–416.

Levin, B. R., F. M. Stewart, and L. Chao, 1977 Resource-limited growth, competition, and predation: a model and experimental studies with bacteria and bacteriophage. Am. Nat. 111: 3–24.

Levin, B. R., S. Moineau, M. Bushman, and R. Barrangou, 2013 The population and evolutionary dynamics of phage and bacteria with CRISPR-mediated immunity. PLoS Genet. 9: e1003312.

Levinson, G., and G. A. Gutman, 1987 Slipped-strand mispairing: a major mechanism for DNA sequence evolution. Mol. Biol. Evol. 4(3): 203–221.

Losos, J. B., 2010 Adaptive radiation, ecological opportunity, and evolutionary determinism. Am. Nat. 175: 623–639.

Lovett, S. T., 2004 Encoded errors: mutations and rearrangements mediated by misalignment at repetitive DNA sequences. Mol. Microbiol. 52: 1243–1253.

MacLean, R. C., 2005 Adaptive radiation in microbial microcosms. J. Evol. Biol. 18: 1376–1386.

McDonald, M. J., S. M. Gehrig, P. L. Meintjes, X. X. Zhang, and P. B. Rainey, 2009 Adaptive divergence in experimental populations of *Pseudomonas fluorescens*. IV. Genetic constraints guide evolutionary trajectories in a parallel adaptive radiation. Genetics 183: 1041–1053.

Michel, A., O. Clermont, E. Denamur, and O. Tenaillon, 2010 Bacteriophage PhiX174's ecological niche and the flexibility of its *Escherichia coli* lipopolysaccharide receptor. Appl. Environ. Microbiol. 76: 7310–7313.

Miller, J. H., 1985 Mutagenic specificity of ultraviolet light. J. Mol. Biol. 182: 45–65.

Mo, J. Y., H. H. Maki, and M. M. Sekiguchi, 1991 Mutational specificity of the *dnaE173* mutator associated with a defect in the catalytic subunit of DNA polymerase III of *Escherichia coli*. J. Mol. Biol. 222: 925–936.

Mortlock, R. P., 1982 Metabolic acquisitions through laboratory selection. Annu. Rev. Microbiol. 36: 259–284.

Nielsen, L., X. Li, and L. J. Halverson, 2011 Cell-cell and cell-surface interactions mediated by cellulose and a novel exopolysaccharide contribute to *Pseudomonas putida* biofilm formation and fitness under water-limiting conditions. Environ. Microbiol. 13: 1342–1356.

Nilsson, M., W. C. Chiang, M. Fazli, M. Gjermansen, M. Givskov *et al.*, 2011 Influence of putative exopolysaccharide genes on *Pseudomonas putida* KT2440 biofilm stability. Environ. Microbiol. 13: 1357–1369.

Ochman, H., 2003 Neutral mutations and neutral substitutions in bacterial genomes. Mol. Biol. Evol. 20: 2091–2096.

Owen, J. G., and D. F. Ackerley, 2011 Characterization of pyoverdine and achromobactin in *Pseudomonas syringae* pv. phaseolicola 1448a. BMC Microbiol. 11: 218.

Paterson, S., T. Vogwill, A. Buckling, R. Benmayor, A. J. Spiers *et al.*, 2010 Antagonistic coevolution accelerates molecular evolution. Nature 464: 275–278.

Poole, A. M., M. J. Phillips, and D. Penny, 2003 Prokaryote and eukaryote evolvability. Biosystems 69: 163–185.

Poon, K. K. H., E. L. Westman, E. Vinogradov, S. Jin, and J. S. Lam, 2008 Functional characterization of MigA and WapR: putative rhamnosyltransferases involved in outer core oligosaccharide biosynthesis of *Pseudomonas aeruginosa*. J. Bacteriol. 190: 1857–1865.

Rainey, P. B., 1999 Adaptation of *Pseudomonas fluorescens* to the plant rhizosphere. Environ. Microbiol. 1: 243–257.

Rainey, P. B., 2005 Bacteria evolve and function within communities: observations from experimental *Pseudomonas* populations, pp. 83–102 in *The Influence of Cooperative Bacteria on Animal Host Biology*, edited by M. McFail-Ngai, B. Henderson, and N. Ruby. Cambridge University Press, Cambridge.

Rainey, P. B., and M. J. Bailey, 1996 Physical and genetic map of the *Pseudomonas fluorescens* SBW25 chromosome. Mol. Microbiol. 19: 521–533.

Rainey, P. B., and K. Rainey, 2003 Evolution of cooperation and conflict in experimental bacterial populations. Nature 425: 72–74.

Rainey, P. B., and M. Travisano, 1998 Adaptive radiation in a heterogeneous environment. Nature 394: 69–72.

Rainey, P. B., A. Buckling, R. Kassen, and M. Travisano, 2000 The emergence and maintenance of diversity: insights from experimental bacterial populations. Trends Ecol. Evol. 15: 243–247.

Rodin, S. N., and V. A. Ratner, 1983a Some theoretical aspects of protein coevolution in the ecosystem "phage-bacteria" I. The problem. J. Theor. Biol. 100: 185–195.

Rodin, S. N., and V. A. Ratner, 1983b Some theoretical aspects of protein coevolution in the ecosystem "phage-bacteria" II. The deterministic model of microevolution. J. Theor. Biol. 100: 197–210.
Rutherford, K., J. Parkhill, J. Crook, T. Horsnell, P. Rice *et al.*, 2000 Artemis: sequence visualization and annotation. Bioinformatics 16: 944–945.
Sambrook, J., E. F. Fritsch, and T. Maniatis, 1989 *Molecular Cloning: A Laboratory Manual*. Cold Spring Harbor Laboratory Press, Cold Spring Harbor, NY.
Schluter, D., 2000 *The Ecology of Adaptive Radiation*. Oxford University Press, Oxford.
Schluter, D., 2009 Evidence for ecological speciation and its alternative. Science 323: 737–741.
Seed, K. D., D. W. Lazinski, S. B. Calderwood, and A. Camilli, 2013 A bacteriophage encodes its own CRISPR/Cas adaptive response to evade host innate immunity. Nature 494: 489–491.
Shin, H., J. H. Lee, H. Kim, Y. Choi, S. Heu *et al.*, 2012 Receptor diversity and host interaction of bacteriophages infecting *Salmonella enterica* serovar Typhimurium. PLoS ONE 7: e43392.
Silby, M. W., A. M. Cerdeño-Tárraga, G. S. Vernikos, S. R. Giddens, R. W. Jackson *et al.*, 2009 Genomic and genetic analyses of diversity and plant interactions of *Pseudomonas fluorescens*. Genome Biol. 10: R51.
Simpson, G. G., 1953 *The Major Features of Evolution*. Columbia University Press, New York.
Spiers, A. J., and P. B. Rainey, 2005 The *Pseudomonas fluorescens* SBW25 Wrinkly Spreader biofilm requires attachment factor, cellulose fibre and LPS interactions to maintain strength and integrity. Microbiology 151: 2829–2839.
Spiers, A. J., S. G. Kahn, J. Bohannon, M. Travisano, and P. B. Rainey, 2002 Adaptive divergence in experimental populations of *Pseudomonas fluorescens*. I. Genetic and phenotypic bases of Wrinkly Spreader fitness. Genetics 161: 33–46.
Spiers, A. J., J. Bohannon, S. M. Gehrig, and P. B. Rainey, 2003 Biofilm formation at the air-liquid interface by the *Pseudomonas fluorescens* SBW25 Wrinkly Spreader requires an acetylated form of cellulose. Mol. Microbiol. 50: 15–27.
Stein, L. D., C. Mungall, S. Shu, M. Caudy, M. Mangone *et al.*, 2002 The generic genome browser: a building block for a model organism system database. Genome Res. 12: 1599–1610.
Stern, A., and R. Sorek, 2010 The phage-host arms race: shaping the evolution of microbes. Bioessays 33: 43–51.
Viswanathan, M., J. J. Lacirignola, R. L. Hurley, and S. T. Lovett, 2000 A novel mutational hotspot in a natural quasipalindrome in *Escherichia coli*. J. Mol. Biol. 302: 553–564.
Wagner, G. P., and J. Zhang, 2011 The pleiotropic structure of the genotype-phenotype map: the evolvability of complex organisms. Nat. Rev. Genet. 12: 204–213.
Wielgoss, S., J. E. Barrick, O. Tenaillon, S. Cruveiller, B. Chane-Woon-Ming *et al.*, 2011 Mutation rate inferred from synonymous substitutions in a long-term evolution experiment with *Escherichia coli*. G3 1: 183–186.
Winsor, G. L., T. Van Rossum, R. Lo, B. Khaira, M. D. Whiteside *et al.*, 2009 Pseudomonas Genome Database: facilitating user-friendly, comprehensive comparisons of microbial genomes. Nucleic Acids Res. 37: D483–D488.
Wolff, E., M. Kim, K. Hu, H. Yang, and J. H. Miller, 2004 Polymerases leave fingerprints: analysis of the mutational spectrum in *Escherichia coli rpoB* to assess the role of polymerase IV in spontaneous mutation. J. Bacteriol. 186: 2900–2905.
Yang, H. J., M. Matewish, I. Loubens, D. G. Storey, J. S. Lam *et al.*, 2000 *migA*, a quorum-responsive gene of *Pseudomonas aeruginosa*, is highly expressed in the cystic fibrosis lung environment and modifies low-molecular-mass lipopolysaccharide. Microbiology 146: 2509–2519.
Zhang, X.-X., and P. B. Rainey, 2007 Construction and validation of a neutrally-marked strain of *Pseudomonas fluorescens* SBW25. J. Microbiol. Methods 71: 78–81.

Communicating editor: J. Lawrence

GENETICS

Supporting Information
http://www.genetics.org/lookup/suppl/doi:10.1534/genetics.113.154948/-/DC1

Adaptive Divergence in Experimental Populations of *Pseudomonas fluorescens*. V. Insight into the Niche Specialist Fuzzy Spreader Compels Revision of the Model *Pseudomonas* Radiation

Gayle C. Ferguson, Frederic Bertels, and Paul B. Rainey

DOI: 10.1534/genetics.113.154948

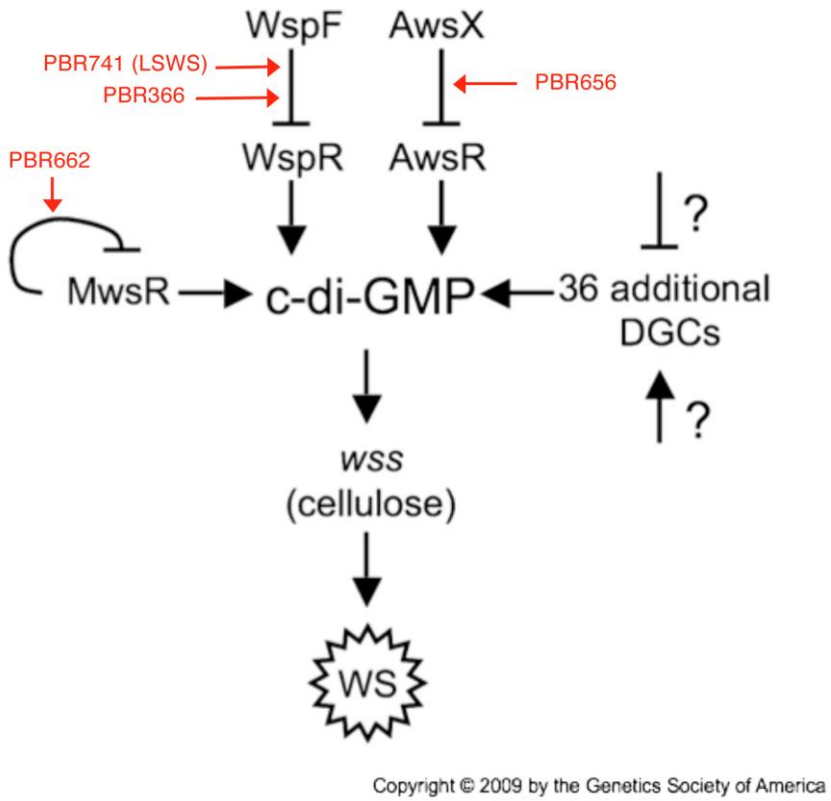

Figure S1 Network diagram of diguanylate cylase (DGC)-encoding pathways underpinning the evolution of the WS phenotype and their regulation (adapted from Figure 2, McDonald et al. 2009). Overproduction of c-di-GMP results in overproduction of cellulose (via activation of enzymes encoded by *wss* genes) and other adhesive factors that form the structural matrix of the WS biofilm (Spiers et al. 2002; Goymer et al. 2006). The ancestral SBW25 genome contains 39 putative DGCs (Silby et al. 2009), each in principle capable of synthesizing the production of c-di-GMP, and yet WS genotypes arise most commonly as a consequence of mutations in just three DGC-containing pathways: Wsp, Aws, and Mws (McDonald et al. 2009). In each instance, the causal mutations are most commonly in the negative regulatory component: *wspF*, *awsX*, and the phosphodiesterase domain of *mwsR*. WS mutant strains used in this study (see Table S1) are indicated in red.

Files S1-S6

Available for download as .mov files at
http://www.genetics.org/lookup/suppl/doi:10.1534/genetics.113.154948/-/DC1

File S1 Growth of FS in a spatially structured KB broth microcosm over a 48-hour period

File S2 Growth of SBW25, FS and WS in spatially structured KB broth microcosms over a 48-hour period

File S3 Flocculation of FS, SBW25 and WS cell suspensions (in KB both) over a 12-hour period

File S4 Growth of FS in spatially structured KB broth microcosms ranging from pH 6.5-8.5 over a 48-hour period

File S5 Flocculation of FS cell suspensions in KB broth of pH 6.5-8.5 over a 12-hour period

File S6 Growth of WS and WS-*fuzY*$_{T443G}$ in spatially structured KB broth microcosms over a 48-hour period

Table S1 Strains and plasmids used in this study

Strain	Relevant genotype [Phenotype]	Source/reference
PBR368	Wild-type *Pseudomonas fluorescens* strain SBW25 [SM]	(RAINEY and BAILEY 1996)
PBR367	'Fuzzy Spreader'; naturally evolved from SBW25; *fuzY*$_{T443G}$ [FS]	(RAINEY and TRAVISANO 1998)
PBR744	SBW25-*fuzY*$_{T443G}$ [FS]	This study
PBR745	SBW25Δ*fuzV*	This study
PBR746	SBW25Δ*fuzW*	This study
PBR747	SBW25Δ*fuzX*	This study
PBR748	SBW25Δ*fuzY* [FS]	This study
PBR749	SBW25Δ*fuzZ*	This study
PBR750	SBW25Δ*fuzVWXYZ*	This study
PBR751	SBW25 with pSX-*fuzY*$_{wt}$ [SM]	This study
PBR752	FS-*fuzY*$_{wt}$ [SM]	This study
PBR753	FS-*fuzY*$_{G443T}$ with pSX-*fuzY*$_{wt}$ [SM]	This study
PBR366	Naturally evolved from SBW25; *wspF*$_{236insGACCGTC}$ [WS]	(RAINEY and TRAVISANO 1998)
PBR754	PBR366 with *fuzY*$_{T443G}$ [fWS]	This study
PBR755	PBR366 with Δ*fuzY* [fWS]	This study
PBR756	PBR754 with pSX-*fuzY*$_{wt}$ [WS]	This study
PBR757	PBR366 with pSX-*fuzY*$_{wt}$ [WS]	This study
PBR656	*awsX*$_{Δ229-261}$ [WS]	(MCDONALD *et al.* 2009)
PBR662	*mwsR*$_{G3055A}$ [WS]	(MCDONALD *et al.* 2009)
PBR758	PBR656 with Δ*fuzY* [fWS]	This study
PBR759	PBR662 with Δ*fuzY* [fWS]	This study
PBR742	PBR367 (FS) with insertion of '*lacZ* between defective prophage genes *pflu1179 and pflu1180,* replacing nucleotides 1312838-1312906 [FS, blue colonies on KBA with X-gal]	This study; (ZHANG and RAINEY 2007)
PBR760	SBW25::Tn*7*-*lacZ* [SM, blue colonies on KBA with X-gal]	This study

Strain	Relevant genotype [Phenotype]	Source/reference
PBR761	FS::Tn*7-lacZ* [FS, blue colonies on KBA with X-gal]	This study
PBR762	SBW25-*fuzY*$_{T443G}$::Tn*7-lacZ* [FS, blue colonies on KBA with X-gal]	This study
PBR763	SBW25Δ*fuzY::*Tn*7-lacZ* [FS, blue colonies on KBA with X-gal]	This study
PBR764	FS-*fuzY*$_{wt}$::Tn*7-lacZ* [SM, blue colonies on KBA with X-gal]	This study
PBR663	LSWS; naturally evolved from SBW25; *wspF*$_{A901C}$ [WS]	(BANTINAKI *et al.* 2007)
PBR741	LSWS::Tn*7-lacZ* [WS, blue colonies on KBA with X-gal]	(MCDONALD *et al.* 2009)
Plasmid		
pSX	oriV, *aacC1*, *bla* (pUCP22); *lacI*q, P*tac*, multiple cloning region (pMMB67EH); with an artificially-introduced ribosome binding site.	(OWEN and ACKERLEY 2011)
pSX-*fuzY*$_{wt}$	pSX with *fuzY* (SBW25) ligated between the *Nde* I and *Bam* HI sites of the multiple cloning region.	This study

Table S2 Full catalogue of *fuzY* mutations within independent FS isolates

isolate [a]	class [b]	nucleotide change [c]	amino acid change [d]	SBW25Φ2 sensitivity [e]
53	aFS	*fuzW*Δ758-896, Δ*fuzX,* Δ*fuzY, fuzZ*Δ1-634	$FuzW_{S253\Delta\ (11)}$, ΔFuzX, ΔFuzY, ΔFuzZ	resistant
8	FS	Δ4 (-1 Fs) [c]	M1Δ (37)	resistant
73	FS	Δ28-33	ΔLQ	resistant
116	FS	G112T (Tv) [c]	E38X	resistant
162	FS	C154T (Ts) [c]	Q52X	resistant
105	FS	Δ193 (-1 Fs)	P66Δ (34)	resistant
104	sFS	268insT (+1 Fs)	F90Δ (4)	resistant
128	FS	276insACGTG	V92Δ (10)	resistant
133	sFS	C288G (Tv)	N96K	resistant
156b	sFS	G352T (Tv)	G118W	resistant
123b	FS	G373T (Tv)	E125X	resistant
145b	sFS	T376A (Tv)	Y126N	resistant
149	FS	C378G (Tv)	Y126X	resistant
115	FS	Δ383 (-1 Fs)	E127Δ (28)	resistant
108	sFS	432insCCTGGCGG	R144Δ (14)	resistant
14	FS	T443G (Tv)	V148G	resistant
18	FS	T443G (Tv)	V148G	resistant
24	FS	T443G (Tv)	V148G	resistant
36	FS	T443G (Tv)	V148G	resistant
97	FS	T443G (Tv)	V148G	resistant
98	FS	T443G (Tv)	V148G	resistant
99	FS	T443G (Tv)	V148G	resistant
102	FS	T443G (Tv)	V148G	resistant
103	FS	T443G (Tv)	V148G	resistant
106	FS	T443G (Tv)	V148G	resistant
118	FS	T443G (Tv)	V148G	resistant

isolate [a]	class [b]	nucleotide change [c]	amino acid change [d]	SBW25Φ2 sensitivity [e]
120	FS	T443G (Tv)	V148G	resistant
124	FS	T443G (Tv)	V148G	resistant
125	FS	T443G (Tv)	V148G	resistant
127	FS	T443G (Tv)	V148G	resistant
136	FS	T443G (Tv)	V148G	resistant
150	FS	T443G (Tv)	V148G	resistant
158	FS	T443G (Tv)	V148G	resistant
159	FS	T443G (Tv)	V148G	resistant
164	FS	T443G (Tv)	V148G	resistant
165	FS	T443G (Tv)	V148G	resistant
166	FS	T443G (Tv)	V148G	resistant
110a	FS	T443G (Tv)	V148G	resistant
110b	FS	T443G (Tv)	V148G	resistant
122b	FS	T443G (Tv)	V148G	resistant
123a	FS	T443G (Tv)	V148G	resistant
151a	FS	T443G (Tv)	V148G	resistant
155a	FS	T443G (Tv)	V148G	resistant
141	FS	Δ462-463 (-2 Fs)	R153Δ (33)	resistant
135	FS	C519G (Tv)	N173K	resistant
65	FS	C565T (Ts)	Q189X	resistant
148	FS	C565T (Ts)	Q189X	resistant
152	FS	Δ568-569 (-2 Fs)	A190Δ (93)	resistant
168	FS	Δ568-569, 568insA (-1 Fs)	Q189Δ (105)	resistant
146	FS	Δ592 (-1 Fs)	P197Δ (97)	resistant
161a	FS	Δ618 (-1 Fs)	G207Δ (87)	resistant
143	FS	G620T (Tv)	G207V	resistant
100a	FS	Δ618-620	L206Δ (75)	resistant
131	FS	C622T (Ts)	R208C	resistant
137	FS	C622T (Ts)	R208C	resistant
117c	FS	C622T (Ts)	R208C	resistant
112	FS	Δ629-760	G210Δ (129)	resistant
56	aFS	A638G (Ts)	K213R	resistant
163	FS	Δ638-639 (-2 Fs)	I212Δ (71)	resistant

isolate [a]	class [b]	nucleotide change [c]	amino acid change [d]	SBW25Φ2 sensitivity [e]
12	sFS	C662A (Tv)	A221E	resistant
140	FS	695insC (+1 Fs)	A232Δ (52)	resistant
5	FS	G712A (Ts)	G238S	resistant
155b	FS	Δ732 (-1 Fs)	A244Δ (50)	resistant
117a	FS	*fuzY*Δ770-1149, *fuzZ*Δ1-220	$FuzY_{T256\Delta\ (220)}$, ΔFuzZ	resistant
68	FS	Δ775-896	R258Δ (84)	resistant
92	FS	Δ779 (-1 Fs)	A259Δ (35)	resistant
145a	sFS	809ins126nt (duplication of 126 nt immediately upstream of insertion point)	Y271Δ (153)	resistant
3	FS	824insTC (+2 Fs)	F275Δ (20)	resistant
129	FS	Δ829-832	D276Δ (17)	resistant
101	FS	T832A (Tv)	W278R	resistant
188b	FS	Δ856-861	ΔGL	resistant
44	FS	G857A (Ts)	G286D	resistant
111a	FS	G857A (Ts)	G286D	resistant
114	FS	Δ862-885	L287Δ (87)	resistant
154	FS	G862C (Tv)	G288R	resistant
132	FS	Δ864 (-1 Fs)	G288Δ (6)	resistant
138	FS	T872C (Ts)	L291P	resistant
153	FS	Δ882-947	G294Δ (67)	resistant
176a	FS	Δ882-947	G294Δ (67)	resistant
151b	FS	897insCC (+2 Fs)	P300Δ (1)	resistant
122a	FS	Δ908-909 (-2 Fs)	I302Δ (37)	resistant
87	FS	945insG (+1 Fs)	G315Δ (25)	resistant
134	FS	945insG (+1 Fs)	G315Δ (25)	resistant
192b	aFS	C947A (Tv)	A316E	resistant
191	FS	951ins Tn *pflu2158*, *pflu4347*, *pflu5832*, or *pflu4873*	G318Δ (10)	resistant
111b	aFS	G953A (Ts)	G318D	resistant
126a	FS	988insT (+1 Fs)	L329Δ (11)	resistant
119	FS	Δ1039 (-1 Fs)	A346Δ (22)	resistant
107	FS	*fuzY*Δ1041-1149, *fuzZ*Δ1-340	$FuzY_{A346\Delta\ (7)}$, ΔFuzZ	resistant
157	FS	C1048T (Ts)	Q350X	resistant

isolate [a]	class [b]	nucleotide change [c]	amino acid change [d]	SBW25Φ2 sensitivity [e]
142	FS	1059insT (+1 Fs)	R353Δ (19)	resistant
156a	FS	C1096T (Ts)	Q366X	resistant
4	aFS	Mutation not found		sensitive
15	aFS	Mutation not found		resistant
34	aFS	Mutation not found		sensitive
43	aFS	Mutation not found		resistant
45	aFS	Mutation not found		resistant
54	aFS	Mutation not found		sensitive
71	aFS	Mutation not found		sensitive
79	aFS	Mutation not found		sensitive
80	aFS	Mutation not found		resistant
179	aFS	Mutation not found		resistant
186	aFS	Mutation not found		resistant
100b	aFS	Mutation not found		sensitive
117b	aFS	Mutation not found		sensitive
126b	aFS	Mutation not found		sensitive
161b	aFS	Mutation not found		sensitive
173b	aFS	Mutation not found		sensitive
176b	aFS	Mutation not found		sensitive
201b	aFS	Mutation not found		sensitive
207b	aFS	Mutation not found		sensitive
214b	aFS	Mutation not found		sensitive

[a] Isolates are ordered by position of mutation (5' to 3' direction).
[b] Mutant class is indicated by color [FS (grey); aFS (purple); sFS (green)]
[c] Different classes of *fuzY* mutations are indicated by color [SNPs (light green); small deletions (yellow); small insertions (pink); large deletions (turquoise); and large insertions (dark green)]; Fs = frameshift; Tv = transversion; Ts = transition.
[d] Bracketed figures indicate the number of amino acid residues from the mutation site until STOP.
[e] All isolates were tested for sensitivity to SBW25Φ2.

Table S3 Evolution of WS types from Independent Fuzzy Spreaders

FS ancestor [a] [*fuzY* mutation]	WS derivative [b] [phenotype]	SBW25Φ2 sensitivity	Mat [c] strength	*fuzY* sequence
FS53 [*fuzW*Δ758-896, Δ*fuzX*, Δ*fuzY*, *fuzZ*Δ1-634]	53.1 [fWS]	resistant	– –	
FS8 [Δ4 (-1 Fs)]	**8.6b [fWS]**	**sensitive**	**–**	Δ4 (-1 Fs), A5T [d]
	8.7a [WS]	sensitive	++	Δ4 (-1 Fs), A5T [d]
	8.8a [WS]	sensitive	++	3insA, G112T(Glu>STOP)
	8.8b [WS]	sensitive	++	Δ4 (-1 Fs), A5T [d]
FS73 [Δ28-33]	73.2 [fWS]	resistant	– –	
FS116 [G112T]	116.7a [fWS]	resistant	– –	
FS162 [C154T]	162.3a [fWS]	resistant	–	
FS105 [Δ193 (-1 Fs)]	**105.2a [fWS]**	**resistant**	**+**	
FS104 [268insT (+1 Fs)]	104.1 [fWS]	resistant	– –	
	104.3a [fWS]	resistant	– –	
FS133 [C288G]	133.2 [fWS]	resistant	–	
FS156b [G352T]	156b.1 [fWS]	resistant	–	
FS123b [G373T]	123b.2 [fWS]	resistant	– –	
FS145b [T376A]	**145b.1 [fWS]**	**resistant**	**+**	
FS115 [Δ383 (-1 Fs)]	115.4 [fWS]	resistant	– –	
FS108 [432insCCTGGCGG]	108.1a [fWS]	resistant	– –	
	108.1b [fWS]	**sensitive**	**+**	Δ433-450 (restores wild-type)
	108.3a [fWS]	**sensitive**	**–**	Δ433-450 (restores wild-type)
	108.3b [SM-like]	sensitive	++	Δ433-450 (restores wild-type)
	108.3d [WS]	sensitive	++	Δ433-450 (restores wild-type)
FS [T443G]	FS.2 [fWS]	resistant	– –	
FS141 [Δ462-463 (-2 Fs)]	141.9a [fWS]	resistant	– –	
FS135 [C519G]	135.1 [fWS]	resistant	– –	
FS65 [C565T]	65.3 [fWS]	resistant	– –	
FS152 [Δ568-569 (-2 Fs)]	152.3 [fWS]	resistant	–	
FS168 [Δ568-569, 568insA (-1 Fs)]	168.2 [fWS]	resistant	–	
FS146 [Δ592 (-1 Fs)]	146.2 [fWS]	resistant	– –	

FS ancestor [a] [*fuzY* mutation]	WS derivative [b] [phenotype]	SBW25Φ2 sensitivity	Mat [c] strength	*fuzY* sequence
FS161a [Δ618 (-1 Fs)]	161a.1 [fWS]	resistant	– –	
	161a.3 [WS]	resistant	– –	
	161a.4 [fWS]	resistant	– –	
FS143 [G620T]	143.3a [WS]	sensitive	++	T620G (restores wild-type)
FS131 [C662T]	131.2 [fWS]	resistant	–	
FS56 [A638G]	56.1 [fWS]	resistant	– –	
FS163 [Δ638-639 (-2 Fs)]	163.2 [fWS]	resistant	–	
FS12 [C662A]	12.1 [fWS]	resistant	– –	
FS140 [695insC (+1 Fs)]	140.3b [SM-like]	sensitive	**– –**	Δ682$_{(-1\ Fs)}$ 694insC$_{(+1\ Fs)}$ (corrects frameshift)
FS5 [G712A]	5.2 [fWS]	resistant	–	
FS117a [*fuzY*Δ770-1149, *fuzZ*Δ1-220]	117a.2 [fWS]	resistant	– –	
FS68 [Δ775-896]	68.1 [fWS]	resistant	–	
FS92 [Δ779 (-1 Fs)]	92.2a [fWS]	resistant	– –	
	92.3 [fWS]	resistant	–	
FS145a [809ins126nt]	145a.1 [fWS]	resistant	– –	
FS3 [824insTC (+2 Fs)]	3.2 [fWS]	resistant	–	
FS129 [Δ829-832]	129.2 [fWS]	resistant	– –	
FS101 [T832A]	**101.4a [WS]**	**resistant**	**++**	
	101.4b [fWS]	resistant	– –	
FS44 [G857A]	44.3 [WS]	sensitive	++	A857G (restores wild-type)
FS132 [Δ864 (-1 Fs)]	132.3 [fWS]	resistant	– –	
FS138 [T872C]	138.3 [WS]	sensitive	++	
FS153 [Δ882-947]	153.2 [fWS]	resistant	–	
FS151b [897insCC (+2 Fs)]	151b.2 [fWS]	resistant	– –	
FS87 [945insG (+1 Fs)]	87.1 [fWS]	resistant	– –	
FS192b [C947A]	192b.1a [fWS]	resistant	– –	
	192b.2a [WS]	**resistant**	**++**	
FS191 [951ins Tn *pflu2158*, *pflu4347*, *pflu5832*, or *pflu4873*]	191.2 [fWS]	resistant	–	

FS ancestor [a] [*fuzY* mutation]	WS derivative [b] [phenotype]	SBW25Φ2 sensitivity	Mat [c] strength	*fuzY* sequence
FS111b [G953A]	111b.1a [fWS]	resistant	– –	
	111b.1b [fWS]	resistant	– –	
FS126a [988insT (+1 Fs)]	126a.2 [fWS]	resistant	–	
FS119 [Δ1039 (-1 Fs)]	119.2 [fWS]	resistant	– –	
FS107 [*fuzY*Δ1041-1149, *fuzZ*Δ1-340]	107.3 [fWS]	resistant	– –	
FS157 [C1048T]	157.3a [fWS]	resistant	– –	
	157.3b [fWS]	resistant	– –	
FS142 [1059insT (+1 Fs)]	142.2 [fWS]	resistant	– –	
FS156a [C1096T]	156a.1a [fWS]	resistant	– –	
	156a.1b [fWS]	**sensitive**	**– –**	T1096C (restores wild-type)
FS15 [no mutation in *fuzY*]	15.1 [fWS]	resistant	–	
FS43 [no mutation in *fuzY*]	43.2a [fWS]	resistant	– –	
	43.2b [fWS]	resistant	–	
FS45 [no mutation in *fuzY*]	45.1a [fWS]	resistant	– –	
	45.1b [fWS]	resistant	– –	
	45.1c [fWS]	resistant	– –	
FS80 [no mutation in *fuzY*]	80.1a [fWS]	resistant	– –	
	80.1b [fWS]	**resistant**	**+**	
FS179 [no mutation in *fuzY*]	179.2b [SM-like]	sensitive	no mat	no mutation in *fuzY*
	179.2b [WS]	sensitive	++	no mutation in *fuzY*
	179.2c [WS]	sensitive	++	no mutation in *fuzY*
FS186 [no mutation in *fuzY*]	**186.2b [WS]**	**resistant**	**+**	

Fifty-six independent FS mutants representing the range of *fuzY* mutational types were propagated for 3-day periods by serial dilution in spatially structured microcosms until the emergence of colony morphologies resembling WS types. WS derivatives were scored for SBW25Φ2 sensitivity and mat strength [as an ability to hold 2mm glass beads, as previously described (RAINEY and RAINEY 2003)]. We sequenced *fuzY* from all phage sensitive isolates to identify reverting or compensatory mutations. The majority of the derived types produced feeble mats (fWS) and remained phage resistant, indicative of the fact that the *fuzY* mutation had neither been reversed nor compensated for by a change restoring functionality to the *fuz* locus; conversely, derived WS types producing strong mats were usually phage sensitive. Exceptions to this general trend are indicated in bold.

[a] Mutant class is indicated by color [FS (grey); aFS (purple); sFS (green)]. Isolates are ordered by position of mutation (5' to 3').
[b] The number of 3-day growth periods prior to detection of each WS isolate is indicated by the number following the decimal point in each isolate name (.1, .2 *etc*).
[c] Mat strength: – – collapsed under the weight of < 5 glass beads; – collapsed under the weight of 5-9 glass beads; + held 10-20 glass beads prior to collapse; ++ held >20 glass beads prior to collapse. Note that typical WS mats uncompromised by *fuzY* mutation are scored as ++.
[d] The A5T SNP in isolates 8.6b, 8.7a and 8.8b creates an in-frame 'GTG' start codon, circumventing the -1 frameshift (Fs) caused by Δ4.

Table S4 Re-evolution of FS and intermediate phenotypes from phage-sensitive FS-derived WS isolates

distant ancestor (FS) [*fuzY* mutation]	immediate ancestor (WS) [*fuzY* mutation]	isolate [a] [phenotype]	SBW25Φ2 sensitivity
FS108 (sFS) [432insCCTGGCGG]	108.1b [Δ432insCCTGGCGG]	B1.1 [SM]	sensitive
		B2.1 [SM]	sensitive
		B4.1 [SM]	sensitive
		B6.1 [SM]	sensitive
		B7.1 [SM]	sensitive
		B8.1a [SM]	sensitive
		B8.1b [Opaque]	sensitive
		B10.1 [SM]	sensitive
		B11.1 [SM]	sensitive
		B2.2a [SM]	sensitive
		B2.2b [WS]	sensitive
		B3.2a [SM]	sensitive
		B3.2b [WS]	sensitive
		B7.2a [SM]	sensitive
		B7.2b [WS]	sensitive
		B8.2a [SM]	sensitive
		B8.2b [WS]	sensitive
		B9.2 [SM]	sensitive
		B12.2 [SM]	sensitive
		B2.3 [FS]	resistant
		B3.3 [aFS]	resistant
		B4.3 [fWS]	resistant
		B5.3 [SM]	sensitive
		B7.3 [aFS]	resistant
		B10.3 [WS]	sensitive
		B12.3 [fWS]	resistant
		B1.4 [FS]	resistant
		B2.4 [FS]	resistant
		B3.4 [aFS]	resistant
		B4.4 [aFS]	sensitive
		B5.4 [FS]	resistant
		B7.4a [aFS]	sensitive
		B7.4b [aFS]	resistant
		B8.4 [aFS]	sensitive
		B10.4 [aFS]	resistant
		B11.4 [FS]	resistant
		B12.4a [FS]	resistant
		B12.4b [aFS]	sensitive
		B12.4c [FS]	resistant
		B12.4d [aFS]	resistant
		B1.5 [FS]	resistant
		B2.5 [FS]	resistant
		B3.5 [FS]	resistant
		B4.5 [FS]	resistant
		B5.5 [FS]	resistant
		B7.5 [FS]	resistant
		B10.5 [FS]	resistant
		B11.5 [FS]	resistant
		B12.5 [aFS]	resistant

distant ancestor (FS) [*fuzY* mutation]	immediate ancestor (WS) [*fuzY* mutation]	isolate [a] [phenotype]	SBW25Φ2 sensitivity
FS140 (FS) [695insC $_{(+1\ Fs)}$]	140.3b [Δ682 $_{(-1\ Fs)}$ 694insC $_{(+1\ Fs)}$]	D9.2 [WS]	sensitive
		D2.3 [fWS]	resistant
		D3.3a [FS]	resistant
		D3.3b [WS]	sensitive
		D4.3 [fWS]	resistant
		D6.3 [fWS]	resistant
		D7.3 [fWS]	resistant
		D8.3 [fWS]	resistant
		D10.3 [fWS]	resistant
		D11.3 [fWS]	resistant
		D12.3 [fWS]	resistant
		D1.4a [fWS]	resistant
		D1.4b [fWS]	resistant
		D2.4a [SM-like]	resistant
		D2.4b [fWS]	resistant
		D3.4a [fWS]	resistant
		D3.4b [fWS]	resistant
		D4.4a [fWS]	resistant
		D4.4b [fWS]	resistant
		D5.4 [fWS]	resistant
		D6.4 [fWS]	resistant
		D7.4a [aFS]	resistant
		D7.4b [fWS]	resistant
		D7.4c [fWS]	resistant
		D8.4a [fWS]	resistant
		D8.4b [fWS]	resistant
		D9.4a [SM-like]	resistant
		D9.4b [fWS]	resistant
		D10.4a [fWS]	resistant
		D10.4b [fWS]	resistant
		D11.4a [fWS]	resistant
		D11.4b [fWS]	resistant
		D12.4a [aFS]	resistant
		D12.4b [fWS]	resistant
		D12.4c [fWS]	resistant
		D4.5 [FS]	resistant
		D6.5 [fWS]	resistant
		D10.5 [aFS]	resistant

distant ancestor (FS) [*fuzY* mutation]	immediate ancestor (WS) [*fuzY* mutation]	isolate [a] [phenotype]		SBW25Φ2 sensitivity
FS156a (FS) [C1096T]	156a.1b [T1096C]	C1.1a	[SM]	sensitive
		C1.1b	[WS]	sensitive
		C1.1c	[FS]	resistant
		C1.1d	[aFS]	sensitive
		C2.1a	[SM]	sensitive
		C2.1b	[WS]	sensitive
		C2.1c	[FS]	resistant
		C2.1d	[aFS]	sensitive
		C3.1a	[SM]	sensitive
		C3.1b	[WS]	sensitive
		C3.1c	[FS]	resistant
		C3.1d	[aFS]	sensitive
		C4.1a	[SM]	sensitive
		C4.1b	[WS]	sensitive
		C4.1c	[FS]	resistant
		C4.1d	[aFS]	sensitive
		C5.1a	[SM]	sensitive
		C5.1b	[WS]	sensitive
		C5.1c	[FS]	resistant
		C5.1d	[aFS]	sensitive
		C6.1a	[SM]	sensitive
		C6.1b	[WS]	sensitive
		C6.1c	[FS]	resistant
		C6.1d	[aFS]	sensitive
		C7.1a	[SM]	sensitive
		C7.1b	[WS]	sensitive
		C7.1c	[FS]	resistant
		C7.1d	[aFS]	sensitive
		C8.1a	[SM]	sensitive
		C8.1b	[WS]	sensitive
		C8.1c	[FS]	resistant
		C8.1d	[aFS]	sensitive
		C9.1a	[SM]	sensitive
		C9.1b	[WS]	sensitive
		C9.1c	[FS]	resistant
		C9.1d	[aFS]	sensitive
		C10.1a	[SM]	sensitive
		C10.1b	[WS]	sensitive
		C10.1c	[FS]	resistant
		C10.1d	[aFS]	sensitive
		C11.1a	[SM]	sensitive
		C11.1b	[WS]	sensitive
		C11.1c	[FS]	resistant
		C12.2a	[SM]	sensitive
		C12.2b	[WS]	sensitive
		C12.2c	[FS]	resistant
		C12.2d	[WS]	sensitive

distant ancestor (FS) [*fuzY* mutation]	immediate ancestor (WS) [*fuzY* mutation]	isolate [a] [phenotype]		SBW25Φ2 sensitivity
SBW25 (SM) [wild-type]	PBR366 [wild-type]	A3.1	[SM]	sensitive
		A6.1	[SM]	sensitive
		A7.1	[SM]	sensitive
		A8.1	[SM]	sensitive
		A10.1	[SM]	sensitive
		A1.2	[SM]	sensitive
		A2.2	[SM]	sensitive
		A4.2	[SM]	sensitive
		A5.2	[SM]	sensitive
		A9.2	[SM]	sensitive
		A11.2	[SM]	sensitive
		A12.2	[SM]	sensitive
		A1.3	[fWS]	resistant
		A2.3	[fWS]	resistant
		A3.3	[fWS]	resistant
		A5.3	[fWS]	resistant
		A7.3	[fWS]	resistant
		A8.3	[fWS]	resistant
		A9.3	[fWS]	resistant
		A10.3	[fWS]	resistant
		A11.3	[fWS]	resistant
		A12.3	[fWS]	sensitive
		A1.4	[aFS]	resistant
		A2.4	[aFS]	resistant
		A3.4	[FS]	resistant
		A4.4	[FS]	resistant
		A7.4	[FS]	resistant
		A10.4	[aFS]	resistant
		A11.4a	[aFS]	resistant
		A11.4b	[WS]	resistant
		A1.5	[FS]	resistant
		A4.5	[FS]	resistant
		A5.5	[FS]	resistant
		A8.5	[FS]	resistant
		A9.5	[FS]	resistant
		A10.5	[FS]	resistant
		A12.5	[FS]	resistant

Twelve replicate populations of each of three distinct FS-derived WS genotypes [plus one archetypal WS genotype (PBR366) derived directly from SBW25 and thus carrying a previously un-mutated *fuzY* gene] were propagated in static microcosms for two successive 3-day periods and three successive 7-day periods by 1:1000 dilution into fresh growth medium at each transfer point. The WS isolate PBR366 was intended as a reference point for time taken to detect FS types derived from WS ancestors. Evolution of FS from WS is expected to require two mutations: one to suppress the constitutive activation of diguanylate cyclases that lead to the over-production of cellulose, and another to inactivate FuzY. SM or fWS 'first step' phenotypes [predicted to carry mutations within either *wsp*, *aws* or *mws* (producing SM) or *fuzY* (producing fWS)] were detected in most populations after one (.1), two (.2) or three (.3) successive transfers and are indicated in red and green, respectively. FS genotypes were detected in 32 of the 48 populations by the end of the three successive 7-day growth periods (.3, .4 or .5) and are indicated in blue. All of the derived FS types were phage resistant. Interestingly, the three distinct FS-derived WS genotypes were strikingly different in their patterns of diversification: 156a.1b populations uniformly diversified into a range of morphotypes, including FS and aFS, after a single 3-day incubation period. In contrast, diversification of 140.3b populations was only detected at the third successive transfer and involved fewer morphotypes. The reasons for these differences are unknown but are likely a consequence of subtly different niche preferences and fitness relative to the derived types.

[a] Isolate names indicate population number (the number preceding the decimal point: 1. - 12.) and the number of successive growth periods prior to detection (number following the decimal point: .1, .2, *etc*).